Neotropical Ichthyology

Original article

https://doi.org/10.1590/1982-0224-2021-0096

Taxonomy and morphology of the skate genus *Atlantoraja* (Rajiformes: Arhynchobatidae)

Correspondence:
Karla D. A. Soares
karlad.soares@yahoo.com.br

Karla D. A. Soares[1], Renan A. Moreira[1], Rafael F. L. da Silva[2] and Ulisses L. Gomes[2]

The skate genus *Atlantoraja* is composed of three species (*A. castelnaui*, *A. cyclophora*, and *A. platana*) which differ from the other Riorajini species, *Rioraja agassizii*, in regards to their clasper features, squamation and presence of a caudal fin. Despite of being distributed along Southwestern Atlantic and commonly captured by fisheries in Brazil, Uruguay and Argentina, detailed accounts on external and internal morphology are scarce and the taxonomic status of *Atlantoraja* species was not revised so far. The aim of this study, therefore, is to review the taxonomy of the genus *Atlantoraja*, updating information on type specimens and clarifying misidentifications among species, and to describe in detail anatomical structures such as neurocranium, visceral arches, pelvic girdle, dermal denticles and teeth. Lectotypes and paralectotypes are designated for *Atlantoraja castelnaui* and *A. cyclophora*. Notes on intraspecific variation within species are also provided. *Atlantoraja cyclophora* and *A. platana* are more similar to each other than to *A. castelnaui* in regards to the squamation (body dorsal surface smooth *vs.* densely covered by prickles) and color pattern of body dorsal surface, position of orbital foramina, overall shape of neucrocranium and body measurements. Lastly, we discuss the morphological differences among species of *Atlantoraja* and recommend the inclusion of characters presented here in future cladistic analyses.

Keywords: Anatomy, *Atlantoraja castelnaui*, *Atlantoraja cyclophora*, *Atlantoraja platana*, Taxonomic review.

Submitted May 31, 2021
Accepted August 20, 2021
by Jennifer Wyffels
Epub December 13, 2021

1 Laboratório de Ictiologia, Departamento de Zoologia, Instituto de Biociências, Universidade de São Paulo, Rua do Matão, Trav. 14, no. 101, 05508-900 São Paulo, SP, Brazil. (KDAS) karlad.soares@yahoo.com.br (corresponding author), (RAM) moreirarandrade@gmail.com.

2 Laboratório de Taxonomia de Elasmobrânquios, Departamento de Zoologia, Instituto de Biologia, Universidade do Estado do Rio de Janeiro, Rua São Francisco Xavier, 524, Maracanã, 20550-900 Rio de Janeiro, RJ, Brazil. (RFLS) scyliorhinus@gmail.com, (ULG) ulisseslg@netscape.net.

Online version ISSN 1982-0224
Print version ISSN 1679-6225

Neotrop. Ichthyol.
vol. 19, no. 4, Maringá 2021

O gênero *Atlantoraja* é composto por três espécies (*A. castelnaui*, *A. cyclophora* e *A. platana*), as quais diferem da outra espécie da tribo Riorajini, *Rioraja agassizii*, em relação a características do clásper, escamas e presença de uma nadadeira caudal. Apesar de serem distribuídas ao longo do Atlântico Sul Ocidental e serem comumente capturadas em atividades pesqueiras do Brasil, Uruguai e Argentina, descrições detalhadas sobre a morfologia externa e interna são escassas e o status taxonômico das espécies de *Atlantoraja* não foi revisado até então. O presente estudo tem como objetivos: revisar a taxonomia do gênero *Atlantoraja*, atualizando as informações sobre espécimes-tipo e elucidando erros de identificação entre as espécies, e descrever estruturas anatômicas, tais como neurocrânio, arcos viscerais, cintura pélvica, dentículos dérmicos e dentes. Lectótipos e paralectótipos são designados para *Atlantoraja castelnaui* e *A. cyclophora*. Notas sobre a variação intraespecífica em cada espécie também são fornecidas. *Atlantoraja cyclophora* e *A. platana* são mais similares entre si do que *A. castelnaui* em relação às escamas (superfície dorsal do corpo lisa *vs*. densamente coberta por dentículos dérmicos), padrão de colorido da superfície dorsal do corpo, posição dos forâmens orbitais, formato geral do neurocrânio e medidas corpóreas. Por fim, comparações morfológicas entre as espécies de *Atlantoraja* são realizadas, recomendando-se a inclusão dos caracteres aqui apresentados em análises cladísticas futuras.

Palavras-chave: Anatomia, *Atlantoraja castelnaui*, *Atlantoraja cyclophora*, *Atlantoraja platana*, Revisão taxonômica.

INTRODUCTION

The genus *Atlantoraja* Menni, 1972 belongs to the tribe Riorajini (McEachran, Dunn, 1998) and is composed of three species, *Atlantoraja platana* (Günther, 1880), *A. cyclophora* (Regan, 1903) and *A. castelnaui* (Miranda Ribeiro, 1907). These species are distributed along southeastern and southern Brazil, Uruguay and Argentina, presenting coastal habits and included in the category "shallow water rajids"; depth distribution records of *A. castelnaui* vary from 5 to 200 m, *A. cyclophora* from 10 to 321 m, and *A. platana* from 10–221 m (McEachran, Miyake, 1990; Cousseau *et al*., 2000; Weigmann, 2016).

Menni (1972) proposed the genus *Atlantoraja* based on clasper characters such as the shape of dorsal terminal 1, number of terminal cartilages and size of dorsal terminal cartilage. Besides the clasper features, *Atlantoraja* species differ from *Rioraja* Whitley, 1939, the other Riorajini genus, in the relative shape of nasal flaps, squamation and occurrence of a caudal fin (Barbosa, Gomes, 1998; Gomes, Paragó, 2005; Soares *et al*., 2021). Species of the genus are also characterized externally by possessing a dark ventral surface with a great number of black mucous pores of the ampullae of Lorenzini (Gomes, Paragó, 2005). Phylogenetic studies analyzing molecular data (Naylor *et al*., 2012; Coelho *et al*., 2020) recovered *A. cyclophora* and *A. platana* as more closely related than to *A. castelnaui*. Contrastingly, Moreira *et al*. (2017) hypothesized a close relationship between *A. castelnaui* and *A. platana* on the basis of clasper characters, but detailed accounts on neurocranium, visceral arches and pelvic girdle are lacking for species of *Atlantoraja*.

Here, we review the taxonomy of *Atlantoraja* species, providing information on the status of type specimens and clarifying previous misidentifications. Detailed descriptions and illustrations of anatomical structures such as neurocranium, visceral arches, pelvic girdle, dermal denticles and teeth are provided as well as notes on intraspecific variation within those species.

MATERIAL AND METHODS

A total of 193 specimens of the three valid species of *Atlantoraja* were examined in this study; 32 of *A. castelnaui*, 110 of *A. cyclophora*, and 51 of *A. platana*. The material examined is preserved in 70% ethanol and deposited in the following institutions: Natural History Museum (BMNH), London; Fundação Universidade do Rio Grande (FURG), Rio Grande; Museu Argentino de Ciencias Naturales "Bernardino Rivadavia" (MACN), Buenos Aires; Museu de Ciências da Pontifícia Universidade Católica do Rio Grande do Sul (MCP), Porto Alegre; Muséum National d'Histoire Naturélle (MNHN), Paris; Museu Nacional do Rio de Janeiro (MNRJ), Rio de Janeiro; Museu de Zoologia, Universidade de São Paulo (MZUSP), São Paulo; Universidade do Estado do Rio de Janeiro (UERJ) and Chondrichthyes Anatomical Collection from Universidade do Estado do Rio de Janeiro (AC.UERJ), Rio de Janeiro; Universidade Santa Úrsula (USU), Rio de Janeiro. The abbreviations TL and DW used throughout the text refer to total length and disc width, respectively. No licenses were needed for the realization of this study.

Of the 193 specimens examined, 22 were measured and 46 dissected. Neurocranium, jaws, hyoid and gill arches, and pelvic skeleton were examined through manual dissections performed with the aid of scissors, scalpels and forceps. In some cases, specimens were placed into hot water (around 60° C) in a solution of potassium carbonate (K_2CO_3) to facilitate the removal of skin and muscles. Photographs of external morphology and skeletal components were taken with a digital camera (Canon Power Shot SX610 HS) and edited with the aid of Adobe Illustrator CC and Adobe Photoshop CS6. Teeth were photographed with the aid of a stereomicroscope. Distributional map for the three species was generated by Google Earth Pro 7.3 and the software QuantumGis 2.18.15.

Measurements and counts follow Hubbs, Ishiyama (1968), McEachran, Compagno (1979) and Leible (1988). The description of the neurocranium was based in Hulley (1972), Leible (1988) and Nishida (1990); visceral skeleton follows Gillis *et al*. (2009), pelvic girdle and fin terminology follows McEachran, Compagno (1979); and dermal denticles and teeth, Leible (1988) and Cappetta (2012), respectively.

Anatomical abbreviations. II, foramen for the optic nerve; **III**, foramen for the oculomotor nerve; **IV**, foramen for the trochlear nerve; **VI**, foramen for the abducens nerve; **1pvr**, first pelvic radial segment; **1pvrc**, condyle for the first pelvic radial segment; **abc**, anterior portion of basibranchial copula; **acvf**, anterior canal vein foramen; **af**, anterior fontanelle; **alt**, alar thorn; **antf**, antorbital facet; **apba**, foramen for the afferent pseudobranchial artery; **bbc**, basibranchial copula; **bh**, basihyal; **bp**, basal plate; **bpt**, basipterygium; **cb I–V** ceratobranchials I–V; **cph**, cerato-pseudohyoid; **eb I–V**, epibranchials I–V; **end**, endolymphatic foramen; **epb**, epiphysial bridge; **eph**,

epi-pseudohyoid; **ethn**, foramen for the passage of the ethmoidal nerve; **flg**, flange; **fm**, foramen *magnum*; **hb II–IV**, hypobranchials II–IV; **hf**, hyomandibular facet; **hmb**, hyomandibula; **hVII**, foramen for the passage of the hyomandibular *ramus* of the *facialis* nerve; **icf**, internal carotid artery foramen; **idt**, interdorsal thorn; **inc**, inner nasal cartilage; **ins**, internasal space; **iot**, interorbital thorn; **ist**, interspiracular thorn; **ja**, jugal arch; **lpbh**, lateral projection of basihyal; **lpp**, lateral pelvic process; **mck**, Meckel's cartilage; **mct**, mediocaudal thorn; **mdt**, middorsal thorn; **mot**, midorbital thorn; **na**, nasal aperture; **nc**, nasal capsule; **nf**, nasal fontanelle; **nut**, nuchal thorn; **obf**, obturator foramen; **oc**, otic capsule; **occ**, occipital condyle; **onc**, outer nasal cartilage; **opc**, opistotic crest; **opd**¸ optic pedicel; **opf**, ophthalmic foramen; **ornc** oronasal canal; **pb I–V**, pharyngobranchials I-V; **pck**, prickles; **peri**, perilymphatic foramen; **pet**, preorbital thorn; **pf**, posterior fontanelle; **pfc**, prefacial commissure; **pib**, pubischia bar; **pnc**, posterior nasal cartilage; **pos**, postorbital process; **pq**, palatoquadrate; **pre**, preorbital process; **prf**, parietal fossa; **prof**, prootic formamen; **ptp**, pterotic process; **pvr**, pelvic radial segments; **ra**, rostral appendix; **rb**, rostral base; **rn**, rostral node; **rs**, rostrum; **rst**, rostral thorn; **sct**, scapular thorn; **soc**, supraorbital crest; **sopf**, superficial ophtalmic foramina; **spt**, spiracular thorn.

RESULTS

Systematic account

Atlantoraja Menni, 1972

Raja (*Atlantoraja*) Menni, 1972:165–173 (original description; type-species by original designation: *Raja cyclophora* Regan, 1903).

Raja. —Miranda Ribeiro, 1907:176–178, figs. XV and XVI (Brazil; only the part referring to *R. cyclophora* and *R. castelnaui*).

Raia. —Garman, 1913:363 (only the part referring to the South American species *R. cyclophora*).

Diagnosis. Species of *Atlantoraja* can be distinguished from *Rioraja* by having a larger disc, with disc width 68.7–82.5% of the total length (*vs*. 62.9–64.3% TL in *Rioraja*); caudal length 40.9–43.7% (*vs*. 51–52.3%); preoral length 11–12.6% (*vs*.12.9–13.5%); mouth width 7.4–8.5% (*vs*. 6.2–7.2%); internasal distance 6.6–8.2% (*vs*. 6–6.5%); snout-vent length 48–52.4% (*vs*. 45.5–46.1%); distance between first and fifth gill openings 13.2–15% and 7.7–9.7%, respectively (*vs*. 11.9–12.5% and 5.7–6.6%); presence of a caudal fin (*vs*. absent); dark spot at the ventral surface of rostrum tip absent (*vs*. present); posterior margin of the anterior nasal flap rounded (*vs*. straight); mucous pore canals numerous and elongated (*vs*. less numerous and rounded); one to three interdorsal thorns (*vs*. one); dark body ventral surface (*vs*. light); component pecten in claspers (*vs*. absent); dorsal terminal 1 cartilage of clasper inverted U-shaped and with no conspicuous proximal shelf (*vs*. triangular and with a conspicuous proximal shelf); dorsal terminal 2 cartilage extended proximally to the lateral margin of the dorsal marginal cartilage (*vs*. not extended proximally).

Atlantoraja castelnaui (Miranda Ribeiro, 1907)

(Figs. 1, 2, 3A, 4A, 5, 6, 13A, D–E, 14A, 15A, 16A, 17A, 18A–B, 19C–D, 20A; Tabs. 1–3)

Raja castelnaui Miranda Ribeiro, 1907:177, fig. XV (original description, syntypes not designated; type locality: Ilha Rasa, Rio de Janeiro, Brazil).

Raja agassizi var. *picta*. —Miranda Ribeiro, 1903:162 (Rio de Janeiro, Brazil; catalogue). —Miranda Ribeiro, 1953:389–418 (type catalogue, Museu Nacional, Rio de Janeiro, Brazil).

Raja castelnaui. —Garman, 1913:361 (systematic account). —Marini, 1929:452 (listed). —Miranda-Ribeiro, 1959:8 (listed). –Ringuelet, Aramburu, 1960:46 (Argentina; catalogue). —Miranda Ribeiro, 1961:5 (Toku Maru; listed). —Figueiredo, 1977:33, fig. 72 (Southern Brazil, catalogue). —Lucena, Lucena, 1981:6–7 (Rio Grande MCP; type catalogue). —Tomás, Tutui, 1996:588 (listed). —Gomes *et. al*., 1997:96 (cervicothoracic synarcual cartilage). —Barbosa, Gomes, 1998:127 (juvenile external morphology). —Gadig, 1998:51 (listed). —Knoff *et. al*., 2001:81 (parasits).

Raja (*Atlantoraja*) *castelnaui*. —Menni, 1972:165–173 (Argentina; catalogue). —Menni, 1973:422–423, fig. 3 (Argentina and Uruguay; catalogue). —Roux, 1979:117 (Brazil and Argentina; listed). —Menni *et al*., 1984:63 (Argentina; catalogue). —Andreata, Séret, 1995:581 (Espírito Santo, Brazil; listed).

Atlantoraja castelnaui. —McEachran, Dunn, 1998:286 (systematic study). —Compagno, 1999:489 (listed). —Mazzoleni, Schwingel, 1999:114 (Itajaí, Santa Catarina, Brazil; listed). —Cousseau *et al*., 2000:14 (Argentina and Uruguay; catalogue). —Menni, Stehmann, 2000:88 (Argentina, Uruguay and Brazil; listed). –Gadig, Gomes, 2003:28 (São Paulo, Brazil; listed). —Bernardes *et al*., 2005:78 (listed). —Compagno, 2005:531 (listed). —Gomes, Paragó, 2005:55–62, figs. 4, 8 and 12 (mucous pore canals). —Oddone *et al*., 2005:70–72 (reproductive biology). —Ebert, Compagno, 2007:116 (listed). —Oddone, Amorim, 2007:43–52 (demographic analysis). —Oddone *et al*., 2008:327 (reproductive biology). —Oddone, Vooren, 2008:5 (egg capsules). —Gomes *et al*., 2010:160–161, fig. 259 (Rio de Janeiro, Brazil; catalogue). —Last *et al*., 2016:749–751 (listed). —Weigmann, 2016:89 (listed). —Moreira *et al*., 2017:1–12 (clasper morphology). —Gomes *et al*., 2019:294-295, fig. 283 (Rio de Janeiro, Brazil; catalogue). —Soares *et al*., 2020:493–500 (scapulocoracoid morphology). —Coelho *et al*., 2020:1–16 (Brazil; ecological niche model). —Silva, Oddone, 2020:1–12 (tooth morphology).

Diagnosis. *Atlantoraja castelnaui* distinguishes from its congeners by presenting a color pattern characterized by a brownish dorsal surface covered with numerous small rounded dark spots distributed randomly (in some cases symmetrically) and extending to the caudal region (*vs*. small dark spots absent in *A. cyclophora* and *A. platana*); adults presenting rough dorsal surface and dermal denticles extending posteriorly (*vs*. dorsal surface smooth and denticles absent in *A. cyclophora* and *A. platana*); eye diameter 3.4–4 times in the inteorbital distance (*vs*. 1.2 times in *A. cyclophora* and 1.6–1.7 times in *A. platana*); dorsal fins closer to the posterior end of caudal fin than to posterior margin

of pelvic fins (*vs.* equidistant to the caudal fin and pelvic fins in *A. cyclophora* and *A. platana*); distance between first gill slits 1.4–1.6 times the distance between last gill slits (*vs.* 1.6–2 times in *A. cyclophora* and 1.6–1.9 times in *A. platana*); ventral terminal cartilage wrench-shaped (*vs*. Y-shape in *A. cyclophora*, flattened in *A. platana*).

External morphology. Proportional morphometrics are presented in Tab. 1. Disc rhomboidal, 1.3 times wider than long. Snout short and obtuse, slightly projecting beyond anterior disc margin and 0.3 times the disc length (Figs. 1–2). Anterior margin of disc strongly concave and posterior margin nearly convex; disc apices broadly rounded. Posterior margin of disc covering the anterior portion of the anterior lobe of pelvic fin. Preorbital length 1.5–1.7 times greater than prenasal length and 1.2–1.3 times the preoral length.

Eyes and spiracles closely set; spiracles projecting obliquely from midline (Fig. 2A). Eye length greater than spiracle length and goes 3.4–4.4 in times the interorbital distance. Anterior nasal flaps broad, not fused medially, about four times the lateral flaps and covering the mouth commissure (Fig. 2B); lateral margin slightly sigmoid, posterior margin rounded and smooth, and inner margin nearly straight. Lateral flaps tube-like, not fringed and outlining the incurrent aperture. Distance between incurrent apertures about equal to distance between mouth corners. Upper jaw convex and lower one nearly straight. Gill openings slitlike and medially situated to the propterygia; first one 1.3–1.7 times greater than fifth. Distance between first gill slits 1.4–1.6 times the distance between fifth gill slits.

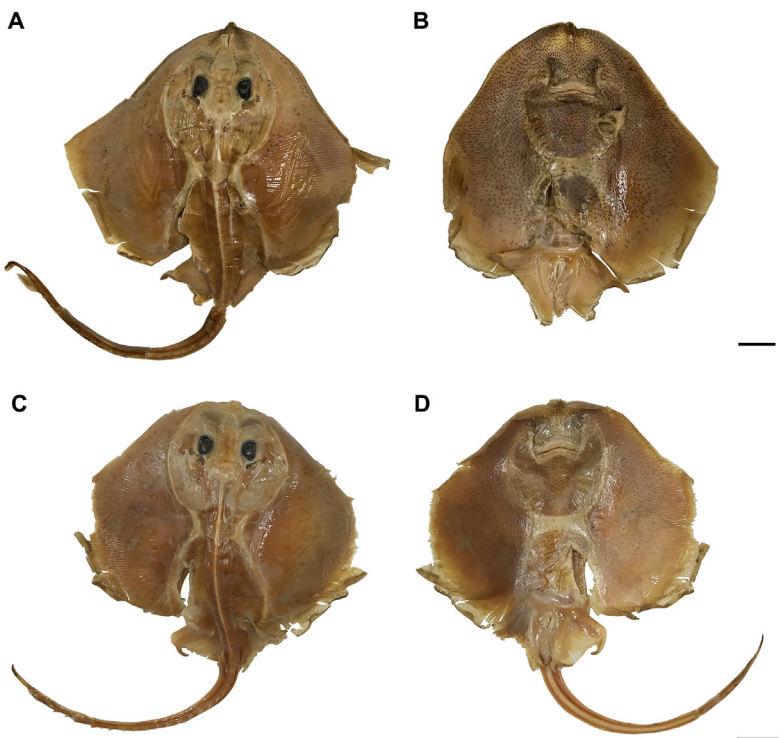

FIGURE 1 | Types of *Atlantoraja castelnaui*. **A**, **B.** MNRJ 608, female, 318.2 mm TL, lectotype; **C**, **D.** MNRJ 19314, male, 226.3 mm TL, paralectotype. Scale bars = 10 cm.

TABLE 1 | Morphometric measurements of six specimens of *Atlantoraja castelnaui* (including the lectotype, MNRJ 608) in millimeters (mm) and proportions of total length (%).

Measurements	MNRJ 608 (mm)	Range (mm)	Range (%)	Mean (mm)	Mean (%)
Total length (TL)	318.2	675–828	100	747.5	100
Disc width	180.3	468–559	67.5–69.3	513.5	68.7
Caudal length	167.2	298–334	40.3–44.0	316.0	42.3
Disc length	142.5	350–444	51.8–53.6	397.0	53.1
Preorbital length	34.9	92–118	13.6–14.2	105.0	14.0
Prenasal length	20.4	54–78	8.0–9.4	66.0	8.8
Internasal distance	21.6	53–62	7.5–7.8	57.5	7.7
Eye diameter	11.9	8–14	1.2–1.7	11.0	1.5
Interorbital distance	14.5	35–48	5.2–5.8	4.5	5.5
Preoral length	35.7	72–99	10.7–11.9	85.9	11.5
Snout-vent length	–	321–397	47.5–47.9	359.0	48.0
Mouth width	24.8	51–68	7.5–8.2	59.5	7.9
Distance from first dorsal fin origin to posterior end of caudal fin	–	110–131	15.8–16.3	120.5	16.1
Distance from posterior margin of pelvic fin to first dorsal fin origin	–	165–195	23.5–24.4	180.0	24.1
First gill slit width	3.9	12–13	1.6–1.8	12.0	1.6
Third gill slit width	–	11–12	1.6–1.8	11.5	1.5
Fifth gill slit width	1.2	7–10	1.0–1.2	8.5	11.4
Distance between first gill slits	36.8	102–118	14.2–15.1	110.0	14.7
Distance between fifth gill slits	28.1	71–74	8.9–10.2	72.5	9.7

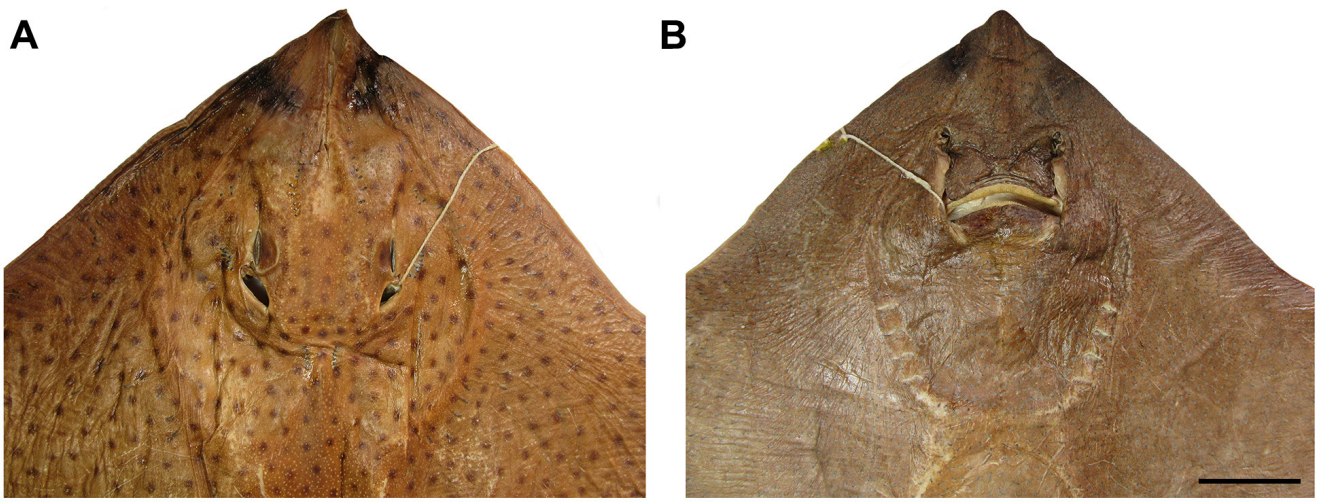

FIGURE 2 | Head region of *Atlantoraja castelnaui*, UERJ 1853, male, 593 mm TL. **A.** Dorsal view. **B.** Ventral view. Scale bar = 10 cm.

Pelvic fins deeply concave outwardly with anterior and posterior portions continuous externally but forming distinct lobes (Fig. 1). Anterior lobe shorter and laterally produced in relation to the posterior lobe; anterior margin nearly straight close to its origin and convex distally. Origin of anterior lobe slightly anterior and ventral to pectoral fin insertion. Distal tips of radials well-marked and prominent along the posterior margin of anterior lobe. Posterior lobe with strongly convex lateral margin and straight inner margin.

Dorsal fins rounded and closely spaced, first one slightly smaller than the second. Distance from posterior margin of pelvic fin to first dorsal fin origin 1.5 times greater than the distance from first dorsal fin origin to posterior end of caudal fin.

Caudal region slender and elongate, 2.3–2.5 times in total length and clearly distinct from disc and tapering from pelvic base to its distal tip (Fig. 4A). Caudal fin with a well-developed dorsal lobe and reduced ventral one, about two times smaller than the second dorsal fin. Caudal fin may be vestigial in juveniles or absent in newborns (Fig. 1A).

Squamation. Skin in juveniles smooth dorsal surface becoming rough in sub-adults and adults due to the development of dermal denticles that extend to the caudal region (*e.g.*, FURG 678, 1270 mm TL). One row of 13 to 22 caudal thorns and two to three interdorsal thorns in juveniles and sub-adults (Fig. 3A; Tab. 2). Number of caudal thorns increasing to 20–25 in adults.

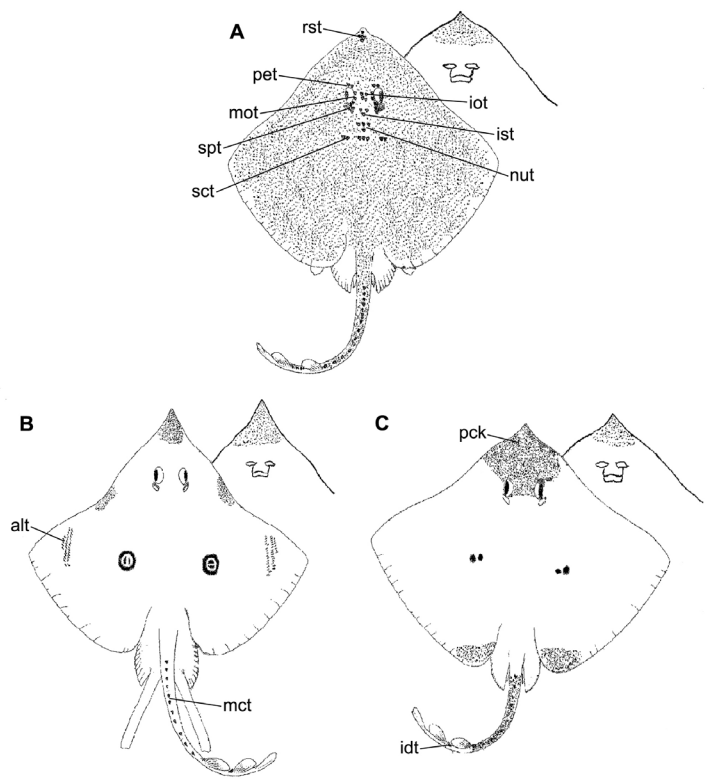

FIGURE 3 | Dorsal squamation of *Atlantoraja* species. **A**, *A. castelnaui*. **B**, *A. cyclophora*. **C**, *A. platana*. Modified from Figueiredo (1977). **alt**, alar thorn; **idt**, interdorsal thorn; **iot**, interorbital thorn; **ist**, interspiracular thorn; **mct**, mediocaudal thorn; **nut**, nuchal thorn; **pck**, prickles; **pet**, preorbital thorn; **rst**, rostral thorn; **sct**, scapular thorn; **spt**, spiracular thorn.

TABLE 2 | Counts of thorns in *Atlantoraja* species. *No adult males of *A. castelnaui* were examined.

Counts	*A. castelnaui*	*A. cyclophora*	*A. platana*
Rostral thorns	5–6	none	none
Preorbital thorns	3–4	none	none
Interorbital thorns	3–4	none	none
Midorbital thorns	3–4	none	none
Postorbital thorns	3–4	none	none
Spiracular thorns	3–4	none	none
Interspiracular thorns	3–4	none	none
Nuchal thorns	6–7	none	none
Scapular thorns	5–6	none	none
Mediocaudal thorns	12–20	4–13	9–15
Interdorsal thorns	2–3	1–3	1–3
Alar thorns	*	88–93	58–76
Alar thorns (rows)	–	6	4

Coloration in alcohol. Dorsal surface of the disc brownish or dark brown, covered with numerous small rounded black blotches (Figs. 2A, 4A). Ontogenetic changes observed with blotches coalesced and less numerous in newborns (Barbosa, Gomes, 1998); some specimens presenting three maculae aggregations in dorsal surface forming a continuous design in which the first (latero-orbital maculae) is located beside the eyes, the second (nuchal maculae) posterior to the eyes and followed by the third (scapular maculae) (Barbosa, Gomes, 1998: 142, fig. 3). Maculae discontinuous and dark blotches symmetrically distributed in larger juveniles; 6 to 7 dark rounded saddles located on the tail. Both maculae and blotches symmetry disappear in subadults and adults.

Neurocranium. Neurocranium long, corresponding to 1.4–1.7 times greater than the nasobasal length and 1.7 times its width (Tab. 3). Rostral cartilage long and stout, its length 1.4–1.7 times in nasobasal length and 3.0–3.4 times greater than its base (Fig. 5). Nasal aperture width 2.7–2.8 times the internasal distance; interorbital distance 2.3–2.4 times the internasal distance. Anterior fontanelle longer than wide, its length 2.4–2.5 times its width and 2.1–2.3 times longer than the posterior fontanelle. Posterior fontanelle 2.3–2.5 times longer than wide. Width across otic capsules 2.0–2.1 times in the neurocranium width. Basal plate width 2.7–4.2 times in the nasobasal length.

Geographical distribution. This species is distributed from Rio de Janeiro, Brazil, to southern Mar del Plata, Argentina (Fig. 6; see also Miranda Ribeiro, 1907, 1923, 1953, 1959; Devincenzi, 1920; Figueiredo, 1977; Roux, 1979; Menni *et al.*, 1984; Andreata, Serét, 1995; Gadig, 1998; Mazzoleni, Schwingel, 1999; Cousseau *et al.*, 2000, 2007; Menni, Stehmann, 2000; Meneses, Paesch, 2003; Bernardes *et al.*, 2005; Coelho *et al.*, 2020). Ruschi (1965) reported a specimen for Espírito Santo State but its identification

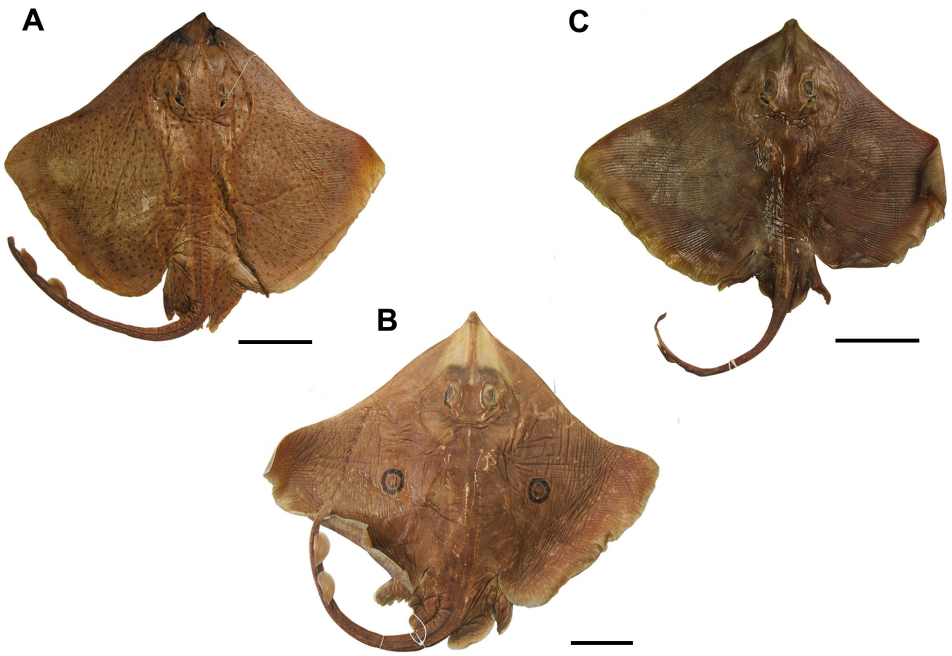

FIGURE 4 | Color pattern of *Atlantoraja* species. **A**, *A. castelnaui*, UERJ 1853, male, 593 mm TL. **B**, *A. cyclophora*, MNRJ 117184, female, 583 mm TL. **C**, *A. platana*, UERJ 1383, male, 372 mm TL. Scale bars = 10 cm.

TABLE 3 | Neurocranial measurements in percentages of nasobasal length (% NL) of male and female specimens of *Atlantoraja castelnaui*.

Measurements	Females (n = 5)		Male (n = 1)
	Range	Mean	
Neurocranium length	145.8–175.0	156.3	123
Rostral cartilage length	56.3–70.8	61.9	–
Neurocranium width	85.0–104.2	95.0	–
Interorbital distance	33.3–38.5	35.0	34.4
Rostral base width	16.7–23.8	20.3	22.9
Anterior fontanelle length	40.0–44.0	41.8	–
Anterior fontanelle width	16.3–17.5	16.8	16.4
Epihyseal bridge length	22.5–26.4	24.2	–
Posterior fontanelle length	18.7–18.8	18.8	–
Posterior fontanelle width	7.5–8.0	8.0	9.8
Width across otic capsules	42.5–50.0	47.0	42.6
Basal plate width	23.8–37.5	33.0	23.0
Nasal aperture width	38.8–45.8	41.9	41.0
Internasal distance	13.8–16.7	15.5	13.1

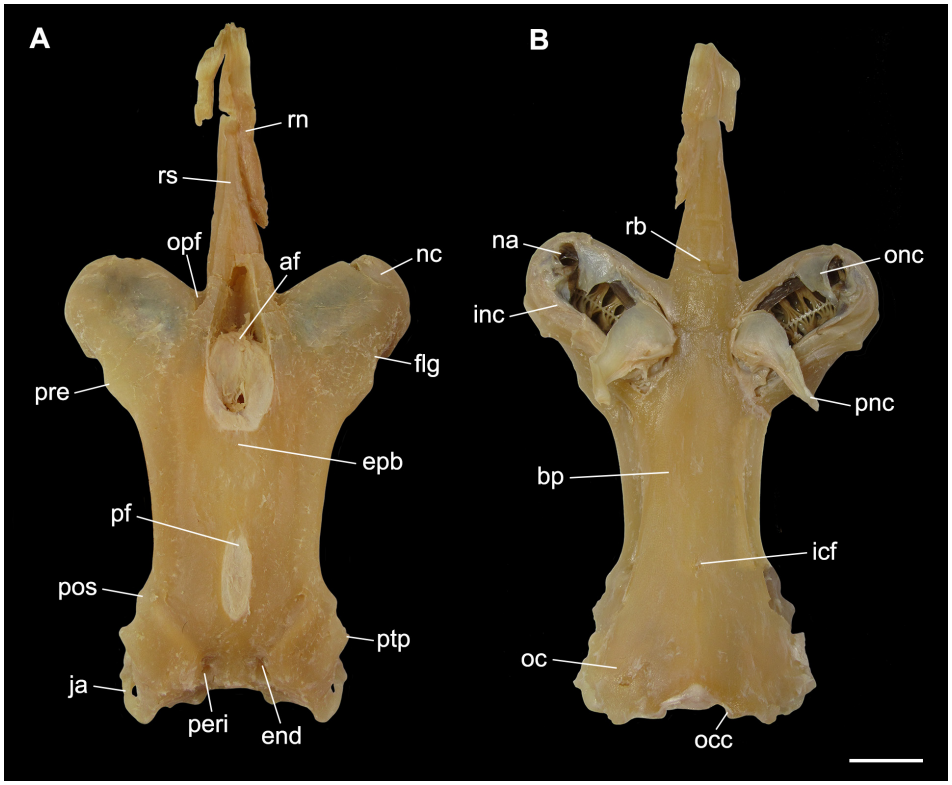

FIGURE 5 | Neurocranium of *Atlantoraja castelnaui*, UERJ 1853, male, 593 mm TL. **A.** Dorsal view. **B.** Ventral view. **af**, anterior fontanelle; **bp**, basal plate; **end**, endolymphatic foramen; **epb**, epiphysial bridge; **flg**, flange; **icf**, internal carotid artery foramen; **inc,** inner nasal cartilage **ja**, jugal arch; **na**, nasal aperture; **nc**, nasal capsule; **oc**, otic capsule; **occ**, occipital condyle; **onc**, outer nasal cartilage; **opf**, ophthalmic foramen; **peri**, perilymphatic foramen; **pf**, posterior fontanelle; **pnc**, posterior nasal cartilage; **pos**, postorbital process; **pre**, preorbital process; **ptp**, pterotic process; **rb**, rostral base; **rn**, rostral node; **rs**, rostrum. Scale bar = 10 mm.

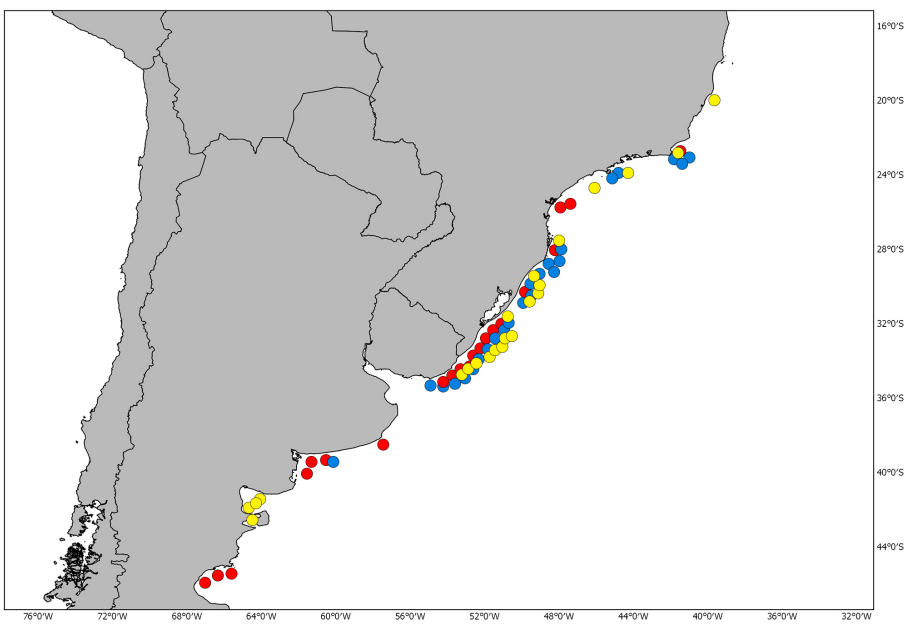

FIGURE 6 | Map showing the geographic distribution of species of *Atlantoraja* based on material examined in this study and literature; *A. castelnaui* (red), *A. cyclophora* (blue), and *A. platana* (yellow).

is not confirmed. It inhabits coastal waters and can be found in depths from 5 to 220 m (Figueiredo, 1977; Vooren, 1997; Bernardes *et. al*., 2005; Oddone, Amorim, 2007; Weigmann, 2016); Lessa *et al*. (1999) reported depths up to 500 m in Brazilian waters but according to Weigmann (2016), this record is questionable.

Biological data. *Atlantoraja castelnaui* is the largest species of the genus, reaching more than 1 m of total length (Miranda Ribeiro, 1923; Figueiredo, 1977; Cousseau *et al*., 2000; Bernardes *et al*., 2005; Oddone, Amorim, 2007; Oddone *et al*., 2008). Largest specimen reported with 1470 mm TL (Weigmann, 2016). Largest female examined measuring 1270 mm TL; largest male 1010 mm TL. Females mature at 1050 mm TL, and males at 910 mm TL (Oddone *et al*., 2008). Newborns measuring 165–180 mm TL. Single egg capsule per oviduct. Both dorsal and ventral surfaces smooth and laterally keeled, varying from 5 to 9 mm in width and from 1.5 to 2.5 mm in height (Oddone *et al*., 2008). No longitudinal striation. Stomach contents composed by Nematoda, Digenea and Acanthocephala (Knoff *et al*., 2001).

Conservation status. This species is categorized as Critically Endangered (CR) (Pollom *et al*., 2020a).

Remarks. *Atlantoraja castelnaui* was identified by Miranda Ribeiro (1903) as a variety of *Raja agassizi* (var. *picta*) and later described under the name *Raja castelnaui* (Miranda Ribeiro, 1907), based on two specimens collected by himself near the coast of Rio de Janeiro (southeastern Brazil). Conversely, Fowler (1910) proposed the name *R. agassizi ribeiroi* for *R. agassizi* var. *picta* and distinguished *Raja castelnaui* from *R. agassizi* var. *picta*. Recently, Menni (1973:423) and Gomes (2002:147) considered *Raja agassizi* var. *picta* as a junior synonym of *Raja castelnaui*. A total of 14 specimens collected during the Annie Expedition Vessel and identified as *Raja agassizi* (including the var. *picta*) by Miranda Ribeiro (1903:162–163) were examined herein. Of these, two specimens, MNRJ 608 and 19314, were identified as *A. castelnaui* based on the dorsal and ventral color pattern, and the description provided by Miranda Ribeiro (1907), and are designated here as lectotype and paralectotype, respectively (Fig. 1). This study recognizes three synonyms for *Atlantoraja castelnaui* (Miranda Ribeiro, 1907): *Raja agassizi* var. *picta* Miranda Ribeiro, 1903; *R. castelnaui* Miranda Ribeiro, 1907 and *R. agassizi riberoi* Fowler, 1910.

Common names. Spotback skate (English), raia-emplastro-pintada (Portuguese).

Material examined. Lectotype. MNRJ 608, female, 318.2 mm TL, between Rio de Janeiro and São Paulo, southeastern Brazil, Annie Expedition Vessel [**Designated herein**]. **Paralectotype.** MNRJ 19314, male, 226.3 mm TL, between Rio de Janeiro and São Paulo, southeastern Brazil, Annie Expedition Vessel [**Designated herein**]. **Argentina.** MACN 396, male, 554 mm TL, 389 mm DW. MACN 2600, male, 180 mm TL, 65 mm DW, 36°25'S 55°54'W. **Brazil.** Rio de Janeiro: MNRJ 568, female, 222 mm TL, 145 mm DW, Ilha Santana. MZUSP uncatalogued, female, 290 mm TL, 192 mm DW, female, 350 mm TL, 248 mm DW, male, 356 mm TL, 240 mm DW. UERJ 692, female, 672 mm TL, 480 mm DW, Copacabana Beach. UERJ 876, male, 247 mm TL, 161 mm DW, Guaratiba. UERJ 877, male, 243 mm TL, 165 mm DW, Guaratiba. UERJ 1890, female, 816 mm TL, 665 mm DW, Ilha Grande. Rio Grande do Sul: FURG 678,

female, 1270 mm TL, 930 mm DW. MOVI 8489, female, 1225 mm TL, 848 mm DW, 29°37'32"S 48°36'01"W. MOVI 8480, female, 1027 mm TL, 772 mm DW, 29°37'32"S 48°36'01"W. Santa Catarina: MCP 964, female, 741 mm TL, 529 mm DW, Garopaba; MCP 8035, male, 1010 mm TL, 705 mm DW, Canto do Grande Beach, Portobelo. MZUSP 190, female, 171 mm TL, 98 mm DW, 28°42'S 48°46'W. São Paulo: AC. UERJ 941, female, 713 mm TL, Ilha da Moela, Guarujá. UERJ 887, female, 205 mm TL, 133 mm DW, female, 184 mm TL, 114 mm DW, between Paranaguá, Paraná, and Ilha do Bom Abrigo, São Paulo. UERJ 1146, female, 165 mm TL, 93 mm DW, Ilha do Bom Abrigo. UERJ 1686, female, 270 mm TL, 180 mm DW, Largo da Moela, Guarujá. UERJ 1628, male, 220 mm TL, 141 mm DW, Santos. UERJ 1629, female, 391 mm TL, 265 mm DW, Santos. UERJ 1687, female, 605 mm TL, 410 mm DW, Largo da Moela, Guarujá. UERJ 1853, male, 598 mm TL, 418 mm DW, Santos. **Uruguay.** MZUSP uncatalogued, female, 281 mm TL, 190 mm DW, 35°19'S 54°13'W. MZUSP 1915, female, 230 mm TL, 147 mm DW, 35°00'S, 54°50'W. MZUSP 9937.1, male, 410 mm TL, 283 mm DW, male, 410 mm TL, 283 mm DW, 29°52'S 49°37'W.AC.UERJ 747, female, 200 mm TL, 133 mm DW (no locality data); AC. UERJ 956, female, 850 mm TL (no locality data); AC. UERJ 958, female, 725 mm TL (no locality data); AC.UERJ 1384, male, 628 mm TL, 433 mm DW (no locality data).

Atlantoraja cyclophora (Regan, 1903)

(Figs. 3B, 4B, 6–9, 13B, F, 14B, 15B, 16B, 17C, 18C–D, 19A–B, 20B; Tabs. 2, 4 and 5)

Raja cyclophora Regan, 1903:60 (original description; type locality: Rio de Janeiro, Brazil).

Raja agassizi var. *meta*. —Miranda Ribeiro, 1903:163 (Annie Vessel). —Miranda Ribeiro, 1953:406 (in part.).

Raja castelnaui. —Miranda Ribeiro, 1907:178, pl. XVI (Rio de Janeiro, Brazil; catalogue). —Garman, 1913:362 (systematic account).

Raja (*Atlantoraja*) *cyclophora*. —Menni, 1972:165–173 (Argentina; catalogue). —Roux, 1979:116 (Brazil and Argentina; listed). —Menni *et al*., 1984:89 (Argentina; catalogue).

Raja cyclophora. —Leigh-Sharpe, 1924: 574 (clasper morphology). —Figueiredo, 1977:32, fig. 71 (Southern Brazil; catalogue). —Lopes, 1989:202 (Rio de Janeiro, Brazil; catalogue). —Begossi, Figueiredo, 1995:712 (Rio de Janeiro, Brazil; catalogue). —Tomás, Tutui, 1996:588 (listed). —Gomes *et al*., 1997:96 (cervicothoracic synarcual cartilage). —Barbosa, Gomes, 1998:127 (juvenile external morphology). —Gadig, 1998: 51, tab. 1 (listed).

Raja (*Atlantoraja*) *ciclophora*. —Bellisio *et al*., 1979:13 (incorrect spelling).

Atlantoraja cyclophora. —McEachran, Dunn, 1998:286 (systematic study). —Mazzoleni, Schwingel, 1999:114 (Itajaí, Santa Catarina, Brazil; listed). —Compagno, 1999:480 (listed). —Cousseau *et al*., 2000:14 (Argentina and Uruguay; catalogue). —Menni, Stehmann, 2000:88 (Argentina, Uruguay and Brazil; listed). —Oddone *et. al*., 2004:1 (egg capsules). —Bernardes *et al*., 2005:79 (listed). —Gomes, Paragó, 2005:55–62, figs. 2, 6 and 10 (mucous pore canals). —Oddone, Vooren, 2005:1096 (reproductive biology). —Oddone, Velasco, 2006:13 (morphometry). —Ebert, Compagno, 2007:116 (listed). —Oddone, Amorim, 2007:43 (demographic analysis). —Oddone,

Vooren, 2008:5 (egg capsules). —Gomes *et al*., 2010: 163–164, fig. 261 (Rio de Janeiro, Brazil; catalogue). —Last *et al*., 2016:751–752 (listed). —Weigmann, 2016:89 (listed). —Moreira *et al*., 2017:1–12 (clasper morphology). —Gomes *et al*., 2019:296, fig. 285 (Rio de Janeiro, Brazil; catalogue). —Soares *et al*., 2020:493–500 (scapulocoracoid morphology). —Coelho *et al*., 2020:1–16 (Brazil; ecological niche model).

Diagnosis. *Atlantoraja cyclophora* distinguishes from its congeners by presenting dark dorsal ocelli on the dorsal surface (*vs*. absent in *A. castelnaui* and inconspicuous in *A. platana*); body dorsal surface smooth and denticles absent (*vs*. rough and dermal denticles extending posteriorly in *A. castelnaui*); eye diameter 1.2 times in the inteorbital distance (*vs*. 3.4–4 times in *A. castelnaui* and 1.6–1.7 times in *A. platana*); dorsal fins equidistant to the posterior end of caudal fin and posterior margin of pelvic fins (*vs*. 1.5 closer to caudal fin in *A. castelnaui*); distance between first gill slits 1.6–2 times the distance between fifth gill slits (*vs*. 1.4–1.6 times in *A. castelnaui*); glans asymmetrically bifurcated and forming the component grip in adult specimens (*vs*. absent in *A. castelnaui* and *A. platana*); ventral terminal cartilage Y-shaped (*vs*. trapezoidal in *A. platana*, wrench-shaped in *A. castelnaui*).

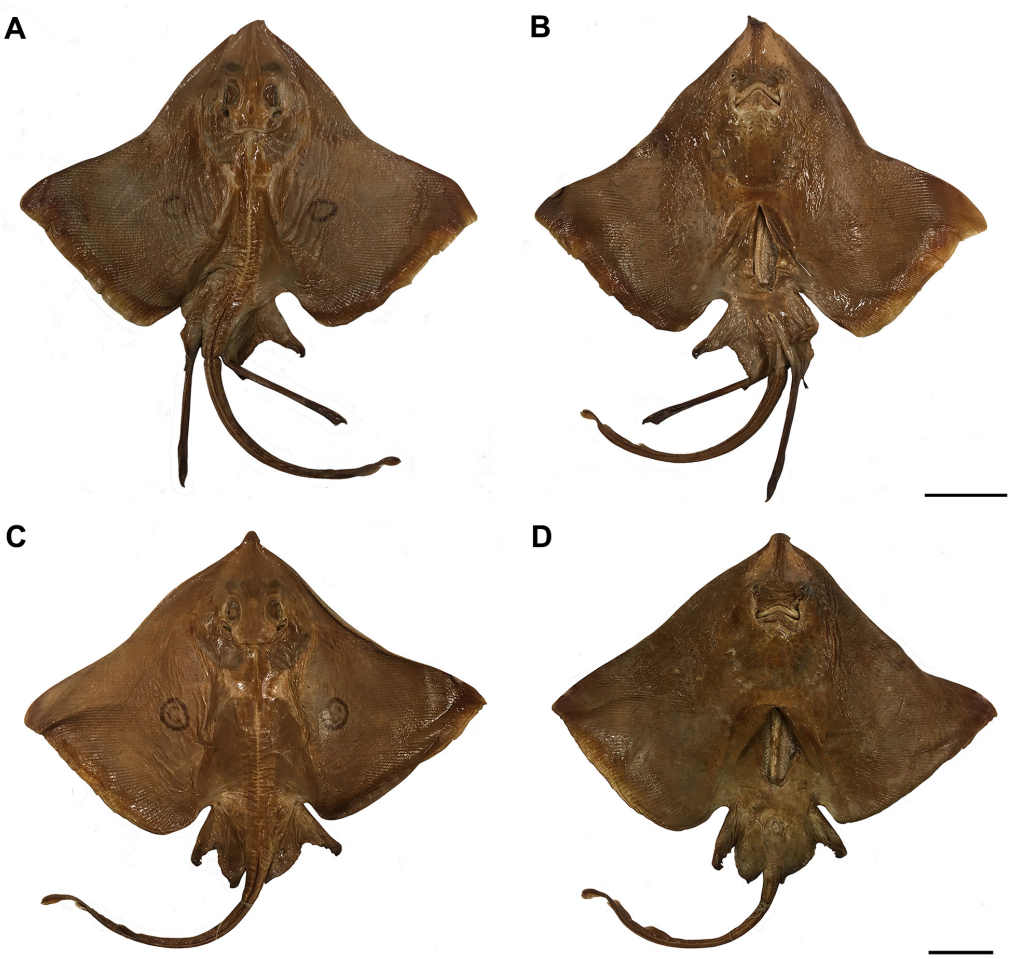

FIGURE 7 | Types of *Atlantoraja cyclophora*. **A**, **B.** BMNH 1903.6.9.134, male, 325 mm DW, lectotype; **C**, **D.** BMNH 1903.6.9.135, female, 430 mm DW, paralectotype. Scale bars = 20 cm.

External morphology. Proportional morphometrics are presented in Table 4. Disc rhomboidal, 1.4 times wider than long. Snout short and obtuse, slightly projecting beyond anterior disc margin and 0.2 times the disc length (Figs. 4B, 7, 8). Anterior margin of disc strongly concave and posterior margin nearly convex; disc apices broadly rounded. Posterior lobe of disc covering the anterior portion of the anterior lobe of pelvic fin. Preorbital length 1.3–1.4 times greater than the prenasal length and 1.1–1.2 times the preoral length.

Eyes and spiracles closely set; spiracles projecting obliquely from midline (Figs. 7A, 7C, 8A). Eye length greater than spiracle length and goes 1.2 times in the interorbital distance. Anterior nasal flaps broad, not fused medially, about four times the lateral flaps and covering the upper lip laterally and mouth commissure (Fig. 8B); lateral margin slightly sigmoid, posterior margin rounded and smooth, and inner margin nearly straight. Lateral flaps tube-like, margins not fringed and outlining the incurrent aperture. Distance between incurrent apertures 0.8–0.9 times the distance between mouth corners. Upper jaw convex and lower one nearly straight. Gill openings slitlike and medially situated to the propterygia; first one 1.1–2 times greater than fifth. Distance between first gill slits 1.6–2 times the distance between fifth gill slits.

TABLE 4 | Morphometric measurements of nine specimens of *Atlantoraja cyclophora* in millimeters (mm) and proportions of total length (%).

Measurements	Range (mm)	Range (%)	Mean (mm)	Mean (%)
Total length (TL)	504–576	100	551	100
Disc width	371–435	73.6–75.5	410.8	74.5
Caudal length	223–256	44.2–44.4	240.9	43.7
Disc length	259–319	51.4–55.3	296.1	53.6
Preorbital length	72–84	14.3–14.6	77.6	14.1
Prenasal length	52–64	10.3–11.1	56.9	10.3
Internasal distance	32–39	6.3–6.8	36.3	6.6
Eye diameter	15–21	3.0–3.6	17.2	3.1
Interorbital distance	18–23	3.6–4.0	20.2	3.7
Preoral distance	61–75	12.1–13.0	69.3	12.6
Snout-vent length	238–285	47.2–49.5	268.4	48.7
Mouth width	38–45	7.5–7.88	41.0	7.4
Distance from first dorsal fin origin to posterior end of caudal fin	96–114	19.0–19.8	107.2	19.4
Distance from posterior margin of pelvic fin to first dorsal fin origin	94–114	18.6–19.8	106.6	19.3
First gill slit width	8–10	1.6–1.7	9.0	1.6
Third gill slit width	7–11	1.4–1.9	9.2	1.7
Fifth gill slit width	4–9	0.8–1.6	5.6	1.0
Distance between first gill slits	63–78	12.5–13.5	72.8	13.2
Distance between fifth gill slits	32–50	6.3–8.4	42.4	7.7

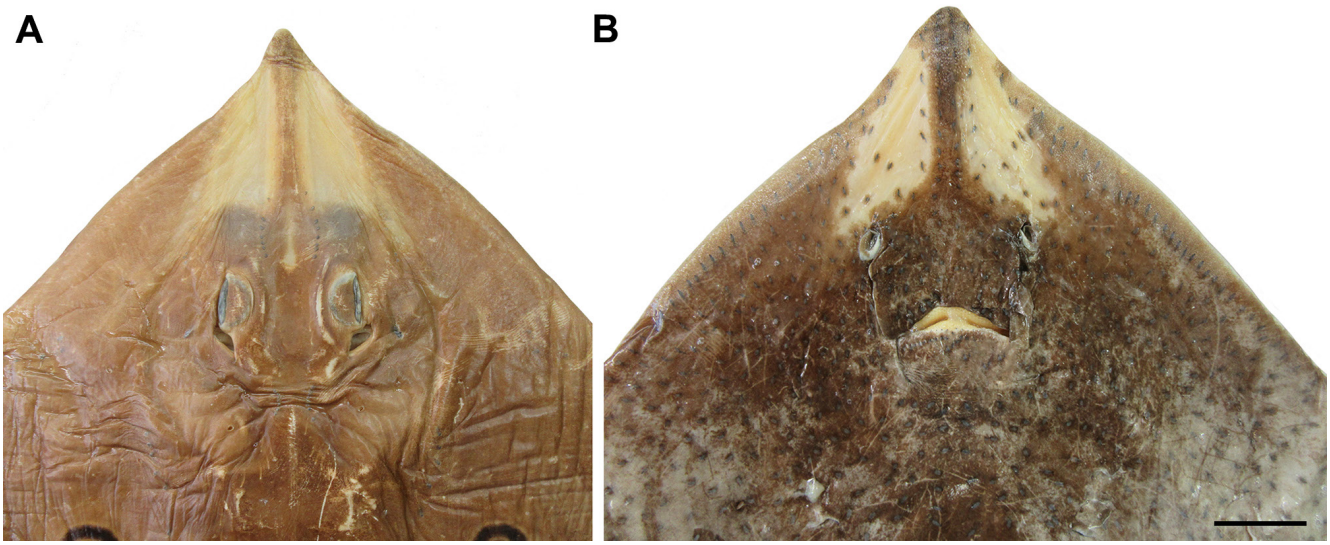

FIGURE 8 | Head region of *Atlantoraja cyclophora*, MNRJ 117184, female, 583 mm TL. **A.** Dorsal view. **B.** Ventral view. Scale bar = 10 cm.

Pelvic fins deeply concave outwardly with anterior and posterior portions continuous externally but forming distinct lobes (Fig. 7). Anterior lobe shorter and laterally produced in relation to the posterior lobe; anterior margin nearly straight close to its origin and convex distally. Origin of anterior lobe slightly anterior and ventral to pectoral fin insertion. Distal tips of radials well-marked and prominent along the posterior margin of anterior lobe. Posterior lobe with strongly convex lateral margin and straight inner margin.

Dorsal fins rounded and closely spaced, first one slightly smaller than the second. Distance from posterior margin of pelvic fin to first dorsal fin origin equal to the distance from first dorsal fin origin to posterior end of caudal fin.

Caudal region slender and elongate, 2.2–2.3 times in total length and clearly distinct from disc and tapering from pelvic base to its distal tip (Figs. 4B, 7). Caudal fin with a well-developed dorsal lobe and reduced ventral one, about two times smaller than the second dorsal fin.

Squamation. Interorbital thorns absent. Alar thorns observed in mature males. Single row of 10 to 15 of median caudal thorns and two to three interdorsal thorns (Fig. 3B; Tab. 2). Females with tail smoother than males due to a small number of lateral prickles.

Coloration in alcohol. A well-defined dorsal ocellus with a light center composed of 1 to 2 concentric dark rings situated on the lateral portions of the dorsal surface of the disc (Fig. 4B, 7A, 7C). Juveniles presenting 6 to 7 dark saddles along the caudal peduncle (Regan, 1903; Miranda Ribeiro, 1907, 1923; Menni, 1973, Figueiredo, 1977; Barbosa, Gomes, 1998). Dark ventral surface with mucous canal pores well-developed, elongate and close to the internasal and interbranchial spaces (Gomes, Paragó, 2005).

Neurocranium. Neurocranium long and corresponding to 1.4–1.9 times greater than the nasobasal length and 1.7–2.1 times its width (Tab. 5). Rostral cartilage long and

stout, its length 1.0–1.5 times in nasobasal length (Fig. 9). Rostral base slender in males and corresponding to 4.1–5.9 times the rostral length *vs.* 3.4–4.0 in females. Rostral appendix on the anterior margin of the rostral cartilage. Nasal aperture width 2.4–3.8 times the internasal distance; interorbital distance 1.9–2.4 times the internasal distance in females and 2.6–2.8 times in males. Anterior fontanelle longer than wide, its length 2.9–4.6 times its width and 1.9–2.5 times longer than the posterior fontanelle. Posterior fontanelle 1.8–2.9 times longer than wide. Width across otic capsules 1.9–2.0 times in the neurocranium width. Basal plate width 2.2–2.7 times in the nasobasal length.

Geographical distribution. This species occurs from Rio de Janeiro, Brazil, to Uruguayan waters and southern of Mar del Plata, Argentina (Fig. 6; see also Evermann, Kendall, 1907; Figueiredo, 1977; Roux, 1979; Menni *et al.*, 1984; Gadig, 1998; Mazzoleni, Schwingel, 1999; Menni, Stehmann, 2000; Cousseau *et al.*, 2000, 2007; Gomes, Gadig, 2003; Meneses, Paesch, 2003; Oddone, Vooren, 2004; Bernardes *et al.*, 2005; Coelho *et al.*, 2020). It inhabits depths between 10 to 321 m (Tomás, Tutui, 1991; Vooren, 1997; Menni, Stehmann, 2000; Bernardes *et al.*, 2005; Oddone, Amorim, 2007; Weigmann, 2016). In Argentinean waters, this species is found in temperatures ranging from 10.3° to 18.5°C at the surface and 6.8° to 18.8°C at the bottom, at depths between 26 to 89 m (Menni, Stehmann, 2000).

TABLE 5 | Neurocranial measurements in percentages of nasobasal length (% NL) of male and female specimens of *Atlantoraja cyclophora*.

Measurements	Females (n = 20)		Males (n = 10)	
	Range	Mean	Range	Mean
Neurocranium length	144.9–200.0	180.6	170.0–191.7	182.0
Rostral cartilage length	68.2–98.4	84.0	70.0–92.0	83.5
Neurocranium width	82.8–100	92.6	82.0–97.2	88.2
Interorbital distance	25.8–35.3	28.8	26.0–33.3	29.8
Rostral base width	17.2–28.6	21.3	11.9–22.2	17.5
Anterior fontanelle length	41.5–49.0	45.1	38.0–45.7	42.7
Anterior fontanelle width	9.0–16.7	12.6	10.0–14.0	11.3
Epiphysial bridge length	20.0–31.7	23.2	22.0–26.1	24.0
Posterior fontanelle length	16.7–25.5	20.0	17.4–22.0	17.9
Posterior fontanelle width	5.8–14.2	8.6	6.0–9.5	8.1
Width across otic capsules	42.4–49.0	45.9	44.0–48.0	45.3
Basal plate width	18.0–28.6	21.8	17.2–21.7	19.6
Nasal aperture width	38.0–45.5	42.2	36.0–45.7	40.5
Internasal distance	10.8–19.0	12.3	10.0–12.0	11.1

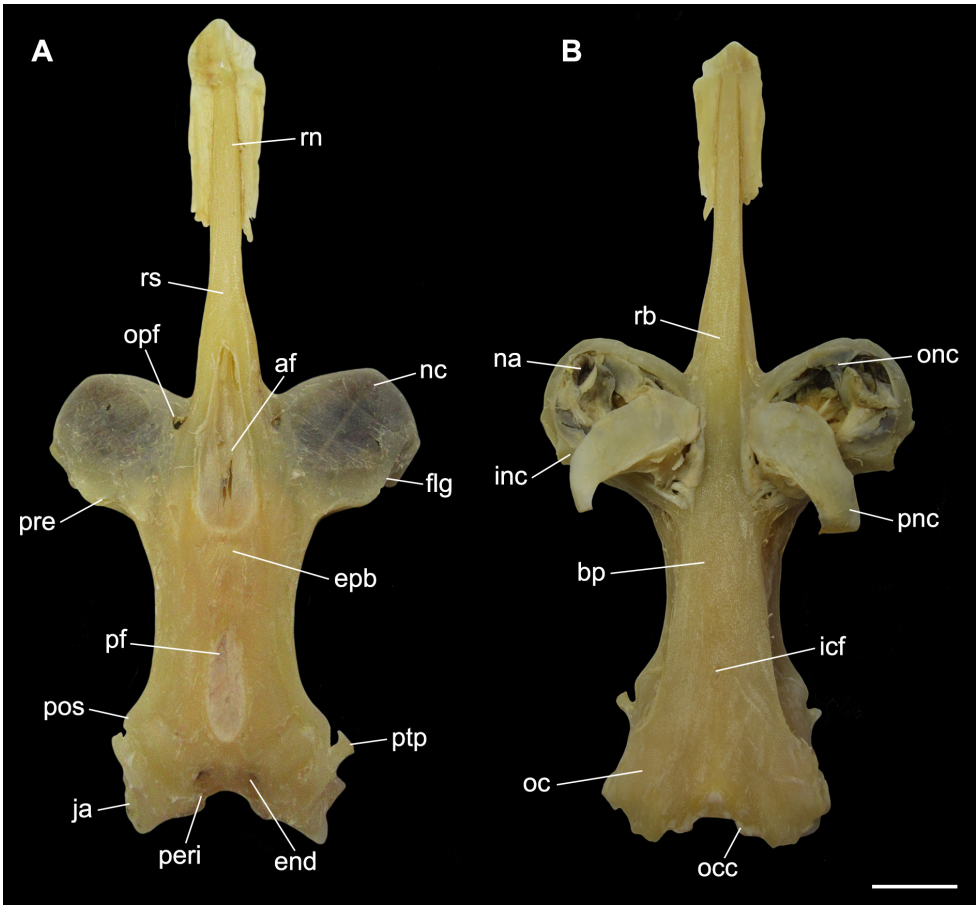

FIGURE 9 | Neurocranium of *Atlantoraja cyclophora*, MNRJ 117184, female, 583 mm TL. **A.** Dorsal view. **B.** Ventral view. **af**, anterior fontanelle; **bp**, basal plate; **end**, endolymphatic foramen; **epb**, epiphysial bridge; **flg**, flange; **icf**, internal carotid artery foramen; **inc**, inner nasal cartilage **ja**, jugal arch; **na**, nasal aperture; **nc**, nasal capsule; **oc,** otic capsule; **occ**, occipital condyle; **onc**, outer nasal cartilage; **opf,** ophthalmic foramen; **peri**, perilymphatic foramen; **pf**, posterior fontanelle; **pnc**, posterior nasal cartilage; **pos**, postorbital process; **pre**, preorbital process; **ptp**, pterotic process; **rb**, rostral base; **rn**, rostral node; **rs**, rostrum. Scale bar = 10 mm.

Biological data. Largest specimen reported with 739 mm TL (Bernardes *et al*., 2005). Largest female examined with 640 mm TL, and largest male examined with 583 mm TL. Newborns measuring 105–115 mm TL. Females become mature at 528 mm TL and males at 485 mm TL (Oddone *et al*., 2008). Dorsal surface of egg capsule symmetrically convex with the highest point situated medially to the edge of a velum markedly convex (Oddone, Vooren, 2008).

Conservation status. This species is categorized as "Endangered" (EN) (Pollom *et al*., 2020b).

Remarks. The first reference to *A. cyclophora* was made by Miranda Ribeiro (1903), who described the species as a variant of *Raja agassizii* (var. *meta*). The time period between this publication and the description of *A. cyclophora* by Regan (1903) consists in only a few months. Thus, the name *Raja agassizii* var. *meta* is considered a senior synonym

of *A. cyclophora*. *Atlantoraja cyclophora* was recorded by Uyeno, Miyake (1983:78) for Suriname and a close relationship with the Amphi-American group of rajiforms (see McEachran, Dunn, 1998) was hypothesized by the presence of a pair of dorsal ocelli. Examining the figure provided by Uyeno, Miyake (1983:78) and comparing with the original description of Bigelow, Schroeder (1961), the Suriname's specimen is markedly different from *A. cyclophora* and corresponds to *Rostroraja cervigoni*. The latter differs from *A. cyclophora* by having a light ventral surface (*vs*. dark in *A. cyclophora*) and the presence of two to three rows of dorsal thorns (*vs*. absent) and tail with three rows of developed thorns, a central and two laterals (*vs*. one row). Despite of the statement of Roux (1979:118) about the probable existence of *R. cervigoni* in Brazilian Northeastern waters, no specimen was ever recorded in Brazil.

Common names. Eyespot skate (English), raia-santa; raia-emplastro-carimbado; raia-emplastro-olhuda (Portuguese).

Material examined. Lectotype. BMNH 1903.6.9.134, male, 325 mm DW, Brazil [**Designated herein**]. **Paralectotype.** BMNH 1903.6.9.135, female, 430 mm DW, Brazil [**Designated herein**]. **Argentina**. MACN 1896, male, 435 mm TL, 325 mm DW, male, 370 mm TL, 292 mm DW. MACN 3052, male, 358 mm TL, 294 mm DW, male, 344 mm TL, 276 mm DW, Puerto Quenquén. MACN 4352, male, 320 mm TL, 247 mm DW, San Antonio. MACN 6173, female, 373 mm TL, 296 mm DW, Puerto Quenquén. **Brazil.** Rio de Janeiro – Ilha Grande: AC.UERJ 753, female, 541 mm TL, 155 mm DW. AC.UERJ.782, male, 485 mm TL, 350 mm DW. AC.UERJ 783, female, 435 mm TL, 330 mm DW. AC.UERJ 785, female, 510 mm TL, 390 mm DW. AC.UERJ 786, female, 495 mm TL, 375 mm DW. AC.UERJ 788, female, 400 mm TL, 320 mm DW. AC.UERJ 789, female, 410 mm TL, 305 mm DW. AC.UERJ.863, male, 163 mm TL, 101 mm DW, male, 148 mm TL, 87 mm. AC.UERJ 1296, female, 435 mm DW. AC.UERJ 1297, female, 422 mm DW. AC.UERJ 1371, male, 23°27'37.6"S 44°09'8"W. AC.UERJ 1372, male, 23°27'40.9"S 44°13'39"W. AC.UERJ 1373, male, 103 mm DW, male, 127 mm DW, 23°27'37.6"S 44°09'8"W). AC.UERJ 1379, male, 542 mm TL, 388 mm DW, 23°27'37.6"S 44°09'8"W). – Rio de Janeiro: MCP 17427, male, 447 mm TL, 332 mm DW. MNHN 1934-22, 4 specimens, 284-570 mm TL. UERJ 740, male, 231 mm TL, 176 mm DW, Maricá. UERJ 748, female, 165 mm TL, 120 mm DW, Ilha de Santana. UERJ 790, female, 106 mm TL, 71 mm DW, Ilha Rasa. UERJ 890, female, 121 mm TL, 91 mm DW, Saquarema. UERJ 894, 4 specimens, 115-216 mm TL, Guaratiba. UERJ 929, 3 specimens, 133-156 mm. Rio Grande do Sul: FURG 661, female, 580 mm TL, 441 mm DW. MOVI 5923, male, 183 mm TL, 136 mm DW, Imbé Beach. UERJ 1848, male, 555 mm TL, 402 mm DW. Santa Catarina - Itajaí: AC.UERJ 611, female, 440 mm TL, 350 mm DW. AC.UERJ 613, female, 525 mm TL, 415 mm DW. AC.UERJ 614, female, 570 mm TL, 460 mm DW. AC. UERJ 617, female, 480 mm TL, 380 mm DW. AC.UERJ 618, female, 380 mm TL, 310 mm DW. AC.UERJ 619, male, 470 mm TL, 345 mm DW. AC.UERJ 622, male, 460 mm TL, 360 mm DW. AC.UERJ 631, male, 505 mm TL, 370 mm DW. AC.UERJ 632, female, 420 mm TL, 320 mm DW. AC.UERJ 633, male, 385 mm TL, 305 mm DW. AC.UERJ 634, female, 545 mm TL, 430 mm DW. AC.UERJ 637, male, 535 mm TL, 395 mm DW. AC.UERJ.784, male, 485 mm TL, 350 mm DW. AC.UERJ 787, male, 510 mm TL, 385 mm DW. AC.UERJ 802, female, 550 mm TL, 420 mm DW. AC.UERJ.803, male, 485 mm TL, 345 mm DW. AC.UERJ.804, male, 458 mm TL, 340 mm DW. AC.UERJ.805, male, 436 mm TL, 332 mm DW. AC.UERJ.806, male, 334 mm TL, 256

mm DW. AC.UERJ. 830, 3 specimens, 340-359 mm TL. UERJ 395, 4 specimens, 210-247 mm TL. UERJ 396, male, 325 mm TL, 257 mm DW. UERJ 397, male, 380 mm TL, 296 mm DW. UERJ 399, female, 517 mm TL, 389 mm DW. UERJ 830, female, 359 mm TL, 270 mm DW. UERJ 1544, female, 245 mm TL, 186 mm DW. - Joatinga: UERJ 378, female, 130 mm TL, 96 mm DW. São Paulo – Santos: AC.UERJ.881, male, 207 mm TL, 153 mm DW. AC. UERJ 949, female, 474 mm TL, 325 mm DW, Ilha Vitória. AC.UERJ 1031, male, 505 mm TL, 374 mm DW. AC.UERJ 1032, male, 467 mm TL, 338 mm DW, Santos. UERJ 895, 4 specimens, 127-186 mm TL, Ilha Bela. UERJ 1625, male, 156 mm TL, 110 mm DW. UERJ 1652, female, 217 mm TL, 159 mm DW, Alcatrazes Archipelago. UERJ 1715, male, 181 mm TL, 140 mm DW, female, 135 mm TL, 99 mm DW, Ubatuba. UERJ 2158, male, 330 mm TL, 470 mm DW. UERJ 2160, female, 570 mm TL, 430 mm DW. No locality data: AC.UERJ 807, female, 420 mm TL, 357 mm DW. AC.UERJ 1259, female. AC.UERJ 1298, female, 581 mm TL. AC.UERJ 1299, male, 557 mm TL. AC.UERJ. 1300, male, 542 mm TL. AC.UERJ. 1301, male, 510 mm TL. AC.UERJ 1302, male, 510 mm TL. AC.UERJ 1303, female, 600 mm TL. AC.UERJ 1304, female, 604 mm TL. AC.UERJ 1305, female, 582 mm TL. AC.UERJ 1306, female, 640 mm TL. AC.UERJ 1307, male, 533 mm TL. AC.UERJ. 1308, male, 510 mm TL. AC.UERJ 1309, female, 587 mm TL. AC.UERJ 1310, male, 583 mm TL. AC.UERJ 1311, female, 587 mm TL. AC.UERJ 1312, male, 517 mm TL. AC.UERJ 1313, female, 490 mm TL. AC.UERJ 1382, male, 510 mm TL. AC.UERJ 1382, male, 510 mm TL, 365 mm DW. AC.UERJ 1382, male, 510 mm TL, 365 mm DW.

Atlantoraja platana (Günther, 1880)

(Figs. 3C, 4C, 6, 10–12, 13C, G, 14C, 15C, 16C, 17B, 18E–F, 19E–F, 20C; Tabs. 2, 6 and 7)

Raja platana Günther, 1880: 11, fig. 3 (original description; type-locality: Rio de La Plata, off Montevideo, Uruguay). —Evermann, Kendall, 1907:69 (listed). —Leigh-Sharpe, 1924:574 (clasper morphology). —Devincenzi, 1920: fig.4 (Uruguay; catalogue). —Miranda Ribeiro, 1961:4 (Rio de Janeiro, Brazil; catalogue). —Menni, 1973:428 (Argentina; catalogue). —Figueiredo, 1977:73 (Southern Brazil; catalogue). —Bellisio *et al*., 1979:13 (Argentina; catalogue). —Lucena, Lucena, 1981:9 (MCP; catalogue). —Gomes *et al*., 1997:96 (cervicothoracic synarcual cartilage). —Barbosa, Gomes, 1998:127 (juvenile external morphology). —Gadig, 1998: 50 (listed).

Raja (Atlantoraja) platana. —Sadowsky, Menni, 1974: 23–32, figs. 1–4 (Argentina; catalogue). —Roux, 1979:117 (Brazil and Argentina; listed). —Menni *et al*., 1984:63 (Argentina; catalogue).

Atlantoraja platana. —McEachran, Dunn, 1998:286 (systematic study). —Compagno, 1999:489 (listed). —Mazzoleni, Schwingel, 1999:114 (Itajaí, Santa Catarina, Brazil; listed). —Cousseau *et al*., 2000: 14 (Argentina and Uruguay; catalogue). —Menni, Stehmann, 2000:88 (Argentina, Uruguay and Brazil; listed). —Gomes, Gadig, 2003:52 (São Paulo, Brazil; listed). —Oddone *et al*., 2004:1 (egg capsules). —Bernardes *et al*., 2005:80 (listed). —Compagno *et al*., 2005:531 (listed). —Gomes, Paragó, 2005:55–62, figs. 3, 7 and 9 (mucous pore canals). —Oddone, Velasco, 2006:13 (reproductive biology). —Ebert, Compagno, 2007:116 (listed). —Oddone, Amorim, 2007:43 (demographic analysis). —Oddone, Vooren, 2008:5 (egg capsules). —Gomes *et al*., 2010:162–163, fig. 260 (Rio de Janeiro, Brazil; catalogue). —Last *et*

al., 2016:753–754 (listed). —Weigmann, 2016:90 (listed). —Moreira *et al*., 2017:1–12 (clasper morphology). —Gomes *et al*., 2019:295, fig. 284 (Rio de Janeiro, Brazil; catalogue). —Soares *et al*., 2020:493–500 (scapulocoracoid morphology). —Coelho *et al*., 2020:1–16 (Brazil; ecological niche model).

Dipturus sp. —Bernardes *et al*., 2005:83 (incorrect identification).

Diagnosis. *Atlantoraja platana* distinguishes from its congeners by having dark spots or inconspicuous ocelli on medial region of pectoral fin dorsal surface (*vs.* well-defined ocelli in *A. cyclophora*; small spots scattered around the body in *A. castelnaui*); dorsal surface smooth and denticles absent (*vs.* rough and dermal denticles extending posteriorly in *A. castelnaui*); eye diameter 1.6–1.7 times in the interorbital distance (*vs.* 1.2 times in *A. cyclophora* and 3.4–4 times in *A. castelnaui*); dorsal fins equidistant to the posterior end of caudal fin and posterior margin of pelvic fins (*vs.* 1.5 closer to caudal fin in *A. castelnaui*); distance between first gill slits 1.6–1.9 times the distance between last gill slits (*vs.* 1.4–1.6 times in *A. castelnaui*); ventral terminal cartilage trapezoidal (*vs.* Y-shape in *A. cyclophora*, wrench-shaped in *A. castelnaui*).

External morphology. Proportional morphometrics are presented in Tab. 6. Disc rhomboidal, 1.3–1.4 times wider than long. Snout short and obtuse, slightly projecting beyond anterior disc margin and 0.1–0.2 times the disc length (Figs. 10–11). Anterior margin of disc strongly concave and posterior margin nearly convex; disc apices broadly rounded. Posterior lobe of disc covering the anterior portion of the anterior lobe of pelvic fin. Preorbital length 1.4–1.8 times greater than the prenasal length and 1.2–1.5 times the preoral length.

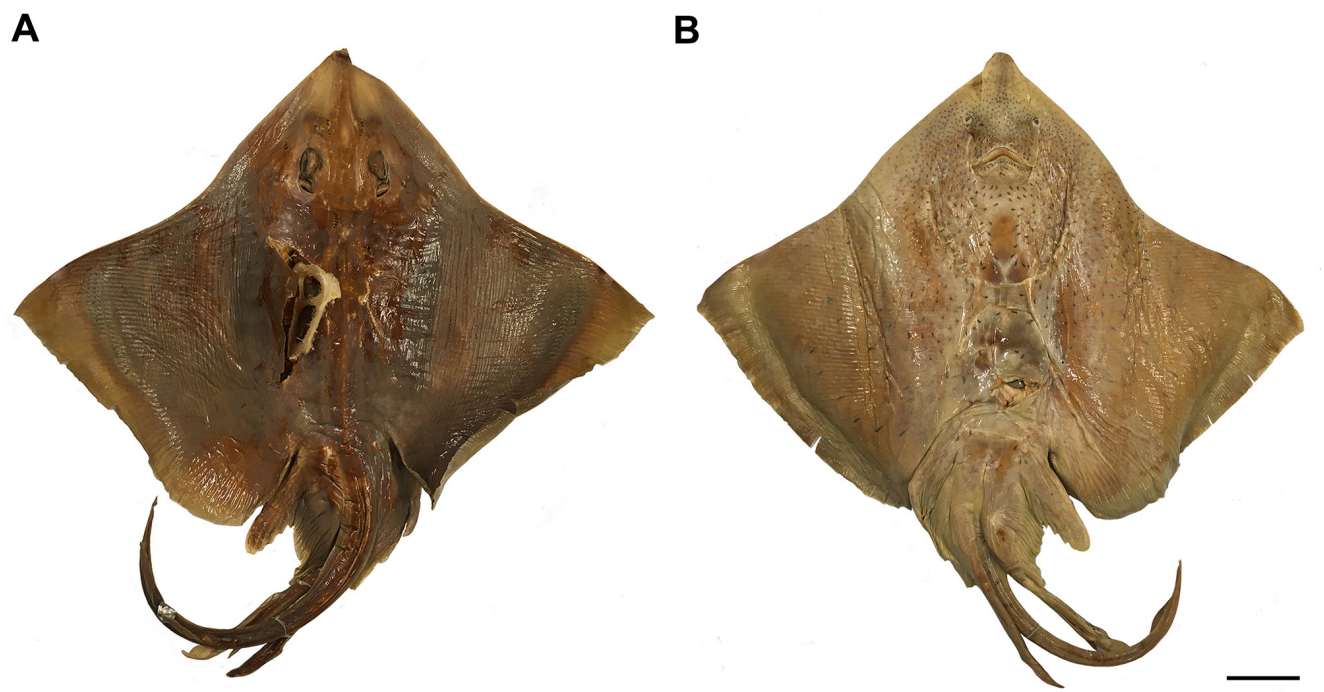

FIGURE 10 | Holotype of *Atlantoraja platana*, BMNH 1879.5.14.411, 647 mm TL. **A.** Dorsal view. **B.** Ventral view. Scale bar = 20 cm.

Eyes and spiracles closely set; spiracles projecting obliquely from midline (Figs. 10A, 11A). Eye length greater than spiracle length and goes 1.6–1.7 times in the interorbital distance. Anterior nasal flaps broad, not fused medially, about four times the lateral flaps and covering the upper lip laterally and mouth commissure (Figs. 10B, 11B); lateral margin slightly sigmoid and notched, posterior margin rounded and smooth, and inner margin nearly straight. Lateral flaps tube-like, margins not fringed and outlining the incurrent aperture. Distance between incurrent apertures 0.9–1.0 times the distance between mouth corners. Upper jaw convex and lower one nearly straight. Gill openings slitlike and medially situated to the propterygia; first one 1.4–1.8 times greater than fifth. Distance between first gill slits 1.6–1.9 times the distance between fifth gill slits.

Pelvic fins deeply concave outwardly with anterior and posterior portions continuous externally but forming distinct lobes (Fig. 10). Anterior lobe shorter and laterally produced in relation to the posterior lobe; anterior margin of pelvic anterior lobe nearly straight close to its origin and convex distally. Origin of anterior lobe slightly anterior and ventral to pectoral fin insertion. Distal tips of radials well-marked and prominent along the posterior margin of anterior lobe. Posterior lobe with strongly convex lateral margin and straight inner margin.

TABLE 6 | Neurocranial measurements in percentages of nasobasal length (% NL) of male and female specimens of *Atlantoraja cyclophora*.

Measurements	Range (mm)	Range (%)	Mean (mm)	Mean (%)
Total length (TL)	533–755	100	681.7	100
Disc width	484–620	82.1–90.8	555.9	82.5
Caudal length	227–303	40.1–42.6	279.1	40.9
Disc length	336–492	63.0–65.1	408.0	640
Preorbital length	77–140	14.4–18.5	101.4	14.8
Prenasal length	55–78	8.2–10.3	65.9	9.7
Internasal distance	44–63	8.2–8.3	50.7	8.2
Eye diameter	15–24	2.8–3.2	19.9	2.9
Interorbital distance	24–40	4.5–5.3	31.6	4.7
Preoral distance	62–95	11.6–12.6	82.1	12.0
Snout-vent length	277–397	52.0–52.6	344.0	52.4
Mouth width	50–63	8.3–9.4	57.3	8.5
Distance from first dorsal fin origin to posterior end of caudal fin	75–159	14.1–21.0	135.7	18.6
Distance from posterior margin of pelvic fin to first dorsal fin origin	94–128	16.9–17.6	114.0	17.2
First gill slit width	9–13	1.7	11.0	1.7
Third gill slit width	8–13	1.5–1.7	11.1	1.6
Fifth gill slit width	5–9	0.9–1.2	7.2	1.1
Distance between first gill slits	81–112	14.8–15.2	101.0	15.0
Distance between fifth gill slits	43–68	8.1–9.0	55.6	8.6

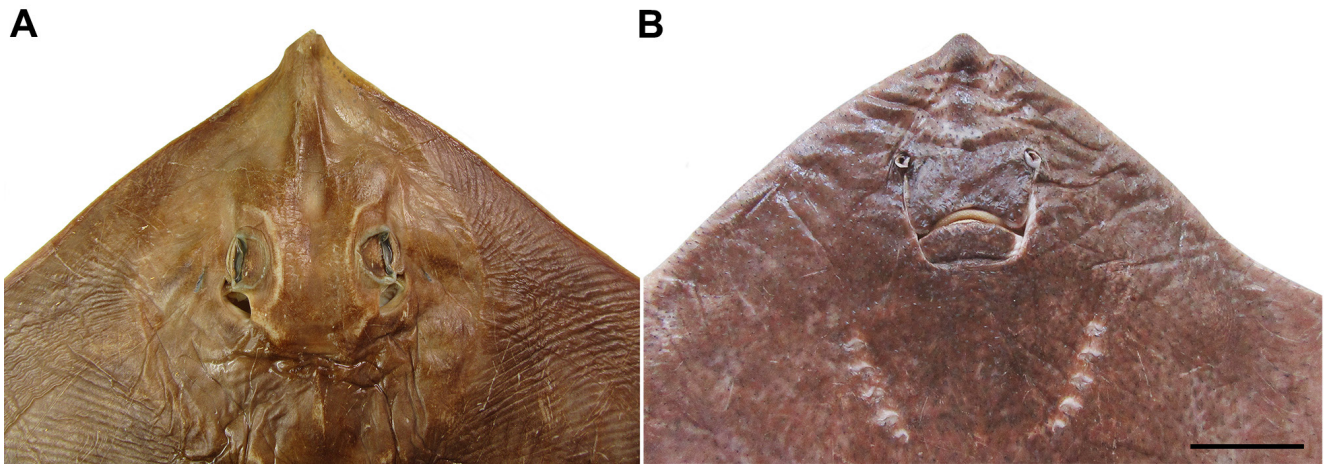

FIGURE 11 | Head region of *Atlantoraja platana*, UERJ 1383, male, 372 mm TL. **A.** Dorsal view. **B.** Ventral view. Scale bar = 10 cm.

Dorsal fins rounded and closely spaced, first one slightly smaller than the second. Distance from posterior margin of pelvic fin to first dorsal fin origin 0.8–1.2 times the distance from first dorsal fin origin to posterior end of caudal fin.

Caudal region slender and elongate, 2.3–2.5 times in total length and clearly distinct from disc and tapering from pelvic base to its distal tip (Figs. 4C, 10). Caudal fin with a well-developed dorsal lobe and reduced ventral one, about two times smaller than the second dorsal fin.

Squamation. Disc without thorns and interorbital prickles well-developed in adults. Rostral thorns more numerous in adult males than in females and juveniles. Most of the thorns concentrated at the caudal peduncle region and forming a single row of 9 to 13 median caudal thorns and one to three interdorsal thorns (Fig. 3C; Tab. 2). Females with lateral caudal thorns along the caudal peduncle and thorns on the posterior margin of pectoral fin.

Coloration in alcohol. Dorsal background surface brown, ventral surface darker (Fig. 4C). Caudal peduncle with 6 to 7 saddles in juveniles and no saddles in adults.

Neurocranium. Neurocranium long and corresponding to 1.1–1.8 times greater than the nasobasal length and 1.3–2.0 times its width (Tab. 7). Rostral cartilage long and stout, its length 1.2–1.9 times in nasobasal length and 2.3–3.0 times rostral base (Fig. 12). Rostral appendix on the anterior margin of the rostral cartilage. Nasal aperture width slightly larger in females (36.0–47.2% NL) than in males (35.4–36.7% NL); in both sexes, nasal aperture corresponds to 2.8–3.1 times the internasal distance; interorbital distance 2.2–2.3 times the internasal distance in females and 2.6–2.7 times in males. Anterior fontanelle longer than wide, its length 2.4–3.3 times its width in females and 3.9–5.8 times in males; anterior fontanelle 2.3–2.5 times longer than the posterior fontanelle. Posterior fontanelle 2.2–2.9 times longer than wide. Width across otic capsules 2.1–4.2 times in the neurocranium width. Basal plate width 4–5 times in the nasobasal length.

Geographical distribution. This species occurs from Rio de Janeiro, Brazil, to southern of Mar del Plata, Argentina (Fig. 6; see also Evermann, Kendall, 1907; Roux, 1979; Gadig, 1998; Lessa *et al*., 1999; Mazzoleni, Schwingel, 1999; Meneses, Paesch, 2003; Menni, Stehmann, 2000; Cousseau *et al*., 2000, 2007; Gomes, Gadig, 2003; Bernardes *et*

TABLE 7 | Neurocranial measurements in percentages of nasobasal length (% NL) of male and female specimens of *Atlantoraja platana*.

Measurements	Females (n = 7)		Males (n = 3)	
	Range	Mean	Range	Mean
Neurocranial length	114.0–180.2	147.5	149.4–169.6	161.2
Rostral cartilage length	53.6–80.2	70.8	49.4–69.6	61.2
Neurocranium width	84.9–92.8	88.9	83.5–84.8	84.0
Interorbital distance	26.7–36.1	32.3	30.4–32.9	32.1
Rostral base width	22.0–27.0	23.9	21.5–24.0	22.8
Anterior fontanelle length	38.9–47.6	43.6	44.3–49.4	46.4
Anterior fontanelle width	11.6–19.4	14.3	7.6–12.7	11.0
Epiphysial bridge length	21.4–27.8	23.4	22.8–28.0	25.4
Posterior fontanelle length	16.3–20.2	18.0	17.7–20.3	18.6
Posterior fontanelle width	5.6–9.3	7.5	7.6	7.6
Width across otic capsules	20.0–44.9	39.1	41.7–43.0	42.2
Basal plate width	19.8–25.0	23.2	20.2–21.5	21.1
Nasal aperture width	36.0–47.2	39.2	35.4–36.7	36.3
Internasal distance	11.6–16.7	14.1	11.4–12.7	11.8

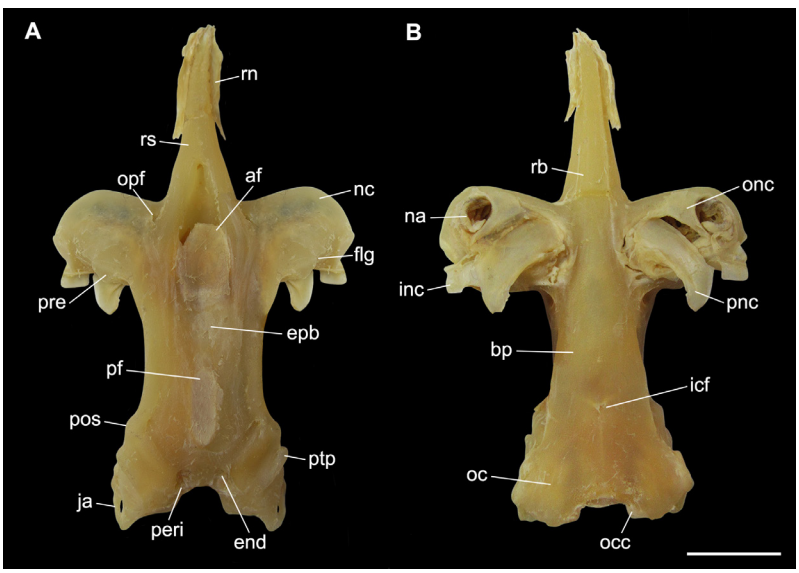

FIGURE 12 | Neurocranium of *Atlantoraja platana*, UERJ 1383, male, 372 mm TL. **A.** Dorsal view. **B.** Ventral view. **af**, anterior fontanelle; **bp**, basal plate; **end**, endolymphatic foramen; **epb**, epiphysial bridge; **flg**, flange; **icf**, internal carotid artery foramen; **inc**, inner nasal cartilage **ja**, jugal arch; **na**, nasal aperture; **nc**, nasal capsule; **oc**, otic capsule; **occ**, occipital condyle; **onc**, outer nasal cartilage; **opf**, ophthalmic foramen; **peri**, perilymphatic foramen; **pf**, posterior fontanelle; **pnc**, posterior nasal cartilage; **pos**, postorbital process; **pre**, preorbital process; **ptp**, pterotic process; **ra**, rostral appendix; **rb**, rostral base; **rn**, rostral node; **rs**, rostrum. Scale bar = 10 mm.

al., 2005; Coelho *et al*., 2020). It inhabits depths between 10-321 m (Figueiredo, 1977; Menni *et al*., 1984; Lessa *et al*., 1999; Vooren, 1997; Menni, Stehmann, 2000; Oddone, Amorim, 2007; Weigmann, 2016).

Biological data. Largest specimen recorded with 910 mm TL (Weigmann, 2016). Largest female examined with 763 mm TL and female with 673 mm TL. Newborns measuring 125–130 mm TL. Females mature at 715 mm TL, and females at 620 mm TL (Oddone, Amorim, 2008). Egg capsules with long posterior horns and dorsal surface asymmetrically convex with the highest point situated toward the anterior end with the edge of the velum straight or slightly concave (Oddone *et al*., 2004). Stomach contents including fishes (Engraulidae, Anguiliformes, *Porichthys*), peneids crustaceans (Stomatopoda, Decapoda, Amphipoda, Isopoda), polychaetas, nematodes. and cephalopods (Menni, Stehmann, 2000).

Conservation status. This species is categorized as "Endangered" (EN) (Pollom *et al*., 2020c).

Common names. La Plata skate (English), raia-emplastro (Portuguese).

Material examined. Holotype. BMNH 1879.5.14.411, 647 mm TL, 503 mm DW, Rio de La Plata, Montevideo, Uruguay, 35°02'S 55°W, 26 m depth. **Argentina.** MACN 976, female, 305 mm TL, 235 mm DW, Puerto Quenquén. **Brazil.** Rio de Janeiro: MZUSP uncatalogued, female, 281 mm TL, 254 mm DW. MZUSP uncatalogued, female, 212 mm TL, 191 mm DW. MZUSP uncatalogued, 14 specimens, 239-575 mm TL. MZUSP 1155.2, male, 135 mm TL, 117 mm DW, 23°43'S 43°55'W. UERJ 1502, female, 162 mm TL, 141 mm DW, male, 241 mm TL, 207 mm DW, Macaé. Rio Grande do Sul: MZUSP uncatalogued, female, 166 mm TL, 139 mm DW, female, 125mm TL, 100 mm DW, 33°08'S 50°45'W. MZUSP 1748, female, 185 mm TL, 163 mm DW, male, 135'mm TL, 112 mm DW, 33°29'S 51°28'W. UERJ 1786, female, 763 mm TL, 623 mm DW, Rio Grande. UERJ 1788, female, 740 mm TL, 606 mm DW, Rio Grande. São Paulo – Santos: AC.UERJ 1027, female, 741 mm TL. AC.UERJ 1034, female, 753 mm TL. AC.UERJ 1035, female, 738 mm TL. AC.UERJ 1037, female, 650 mm TL. AC.UERJ 1039, male, 674 mm TL. AC.UERJ 1040, male, 660 mm TL. AC.UERJ 2162, female, 530 mm TL, 440 mm DW. AC.UERJ 1385, male, 683 mm TL, 537 mm DW. UERJ 2161, male, 657 mm TL, 530 mm DW. UERJ 2162, female, 530 mm TL, 440 mm DW. UERJ 1849, female, 739 mm TL, 577 mm DW. UERJ 1850, male, 666 mm TL, 525 mm DW. UERJ 2161, male, 657 mm TL, 530 mm DW. UERJ 2162, female, 530 mm TL, 440 mm DW. Santa Catarina: AC.UERJ 761, female, 430 mm TL, 370 mm DW, Itajaí. MZUSP 2245, male, 181 mm TL, 155 mm DW, 27°02'S 47°42'W. **Uruguay.** MZUSP uncatalogued, 9 specimens, 161-352 mm TL, 31°24'S 50°12'W. MZUSP 1727, male, 328 mm TL, 287 mm DW, 31°19'S 50°22'W. No locality data: AC.UERJ 1383, male, 370 mm TL, 313 mm DW. MZUSP uncatalogued, male, 469 mm TL, 452 mm DW. MZUSP uncatalogued, 4 specimens, 196-206 mm TL. MZUSP 1155.1, female, 159 mm TL, 156 mm DW. MZUSP 1155.3, male, 130 mm TL, 106 mm DW. UERJ 1785, female, 705 mm TL, 556 mm DW.

Comparative morphology of *Atlantoraja* species

Dermal denticles. Dorsal surface of body (including head region) densely covered by prickles and thorns in *A. castelnaui* while smoother in *A. cyclophora* and *A. platana* (Figs. 3 and 13). Bigelow, Schroeder (1953) described the presence of three rows of thorns in the tail region of *A. castelnaui* but only one row was found surrounded by prickles in the specimens examined (Figs. 13D, E). Rostral, preorbital, interorbital and midorbital, postorbital, spiracular, interspiracular, nuchal, scapular and middorsal thorns present only in *A. castelnaui*, more developed in adult individuals. Adult and subadult male specimens of all three species with alar thorns; absent in females.

Neurocranium. The neurocranium of the three *Atlantoraja* species is dorsoventrally compressed and constricted at the orbital region (Figs. 14–16). Rostrum long and stout, tapering and extending anteriorly to the anterior tip of disc. Rostral appendix longer than wide, extending posteriorly to half-length of the rostrum. Greatest width of neurocranium at the level of nasal capsules.

Nasal capsule thin-walled and varying from strongly oblique in *A. castelnaui*, slightly oblique in *A. cyclophora* to perpendicular in relation to the anteroposterior axis in *A. platana* (Figs. 14–15). Foramen for the passage of the ethmoidal nerve situated on the anterodorsal surface of the nasal capsule, close to the rostral base. Antorbital facet lies on the lateral surface of the nasal capsule, close to its posterior margin, and articulating to the antorbital cartilage; smaller in *A. cyclophora* than in *A. castelnaui* and *A. platana*

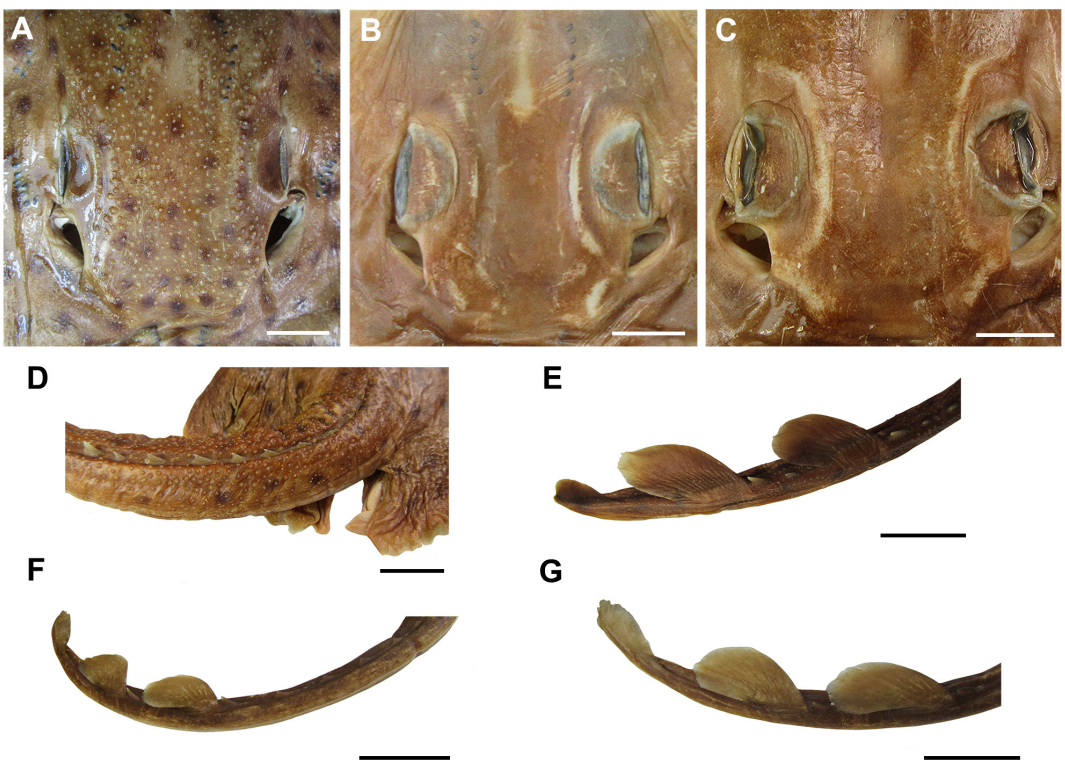

FIGURE 13 | Squamation of *Atlantoraja* species, dorsal body surface. **A**, head, **D**, caudal anterior region and **E**, caudal posterior region of *A. castelnaui*, UERJ 1853, male, 593 mm TL. **B**, head and **F**, caudal region of *A. cyclophora*, MNRJ 117184, female, 583 mm TL. **C**, head and **G**, caudal region of *A. platana*, UERJ 1383, male, 372 mm TL. Scale bars = 20 mm.

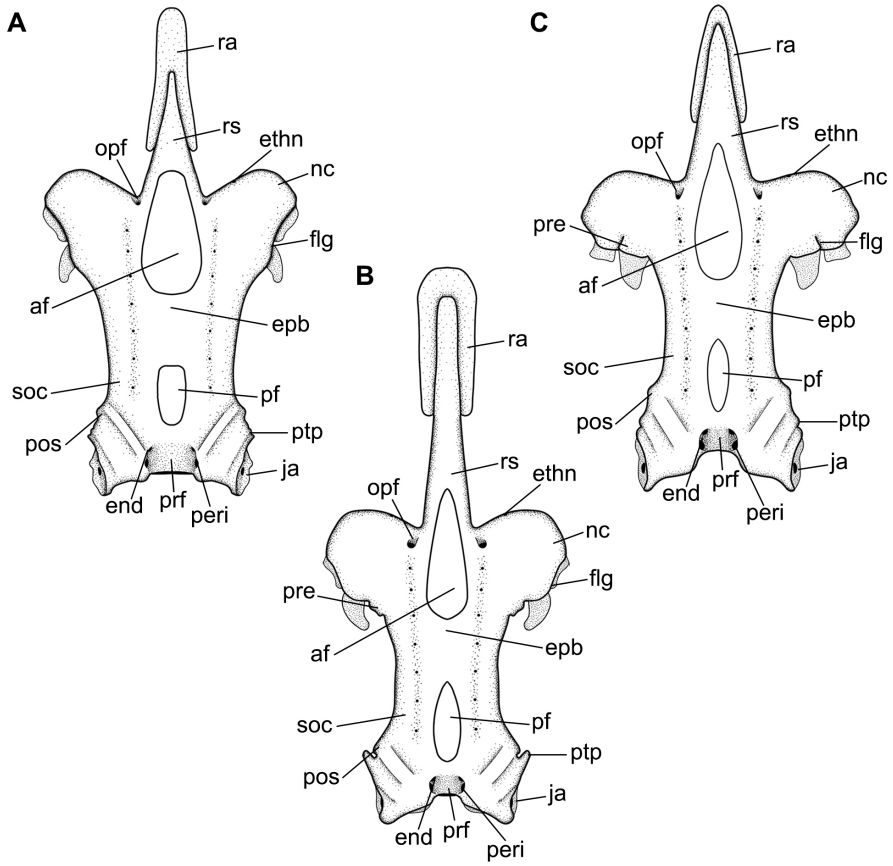

FIGURE 14 | Neurocranium of *Atlantoraja* species, dorsal view. **A**, *A. castelnaui*, UERJ 1853, male, 593 mm TL. **B**, *A. cyclophora*, MNRJ 117184, female, 583 mm TL. **C**, *A. platana*, UERJ 1383, male, 372 mm TL. **af**, anterior fontanelle; **end**, endolymphatic foramen; **epb**, epiphysial bridge; **ethn**, foramen for the passage of the ethmoidal nerve; **flg**, flange; **ja**, jugal arch; **nc**, nasal capsule; **opf**, ophthalmic foramen; **peri**, perilymphatic foramen; **pf**, posterior fontanelle; **pos**, postorbital process; **pre**, preorbital process; **prf**, parietal fossa; **ptp**, pterotic process; **ra**, rostral appendix; **rs**, rostrum; **soc**, supraorbital crest.

(Fig. 16). Flange (*sensu* McEachran, Miyake, 1990) present as a crest that runs dorsally from the nasal capsule to the preorbital process. Nasal aperture wide and extending throughout the nasal fontanelle. Outer nasal cartilage triangular and long, dividing incurrent and excurrent apertures. Internal nasal cartilage wide, running laterally and distally broad and rectangular in shape; it originates from the nasal fontanelle, adjacent to the internasal septum, dorsal and attached to the posterior nasal cartilage medially. Posterior nasal cartilage broad anteriorly, tapering posteriorly and curved distally; this cartilage is oblique in relation the anteroposterior axis, with posterior tip more laterally situated than the anterior one (Fig. 15).

Cranial roof extends from the posterior margin of the anterior fontanelle to the parietal fossa, slightly posterior to the posterior fontanelle and limited laterally by the supraorbital crest (Fig. 14). Its anterior region is broader in *A. castelnaui* in comparison to *A. cyclophora* and *A. platana*. Anterior fontanelle spindle-shaped, beginning at the posterior fourth of the rostral cartilage in *A. cyclophora* and *A. platana* and at the

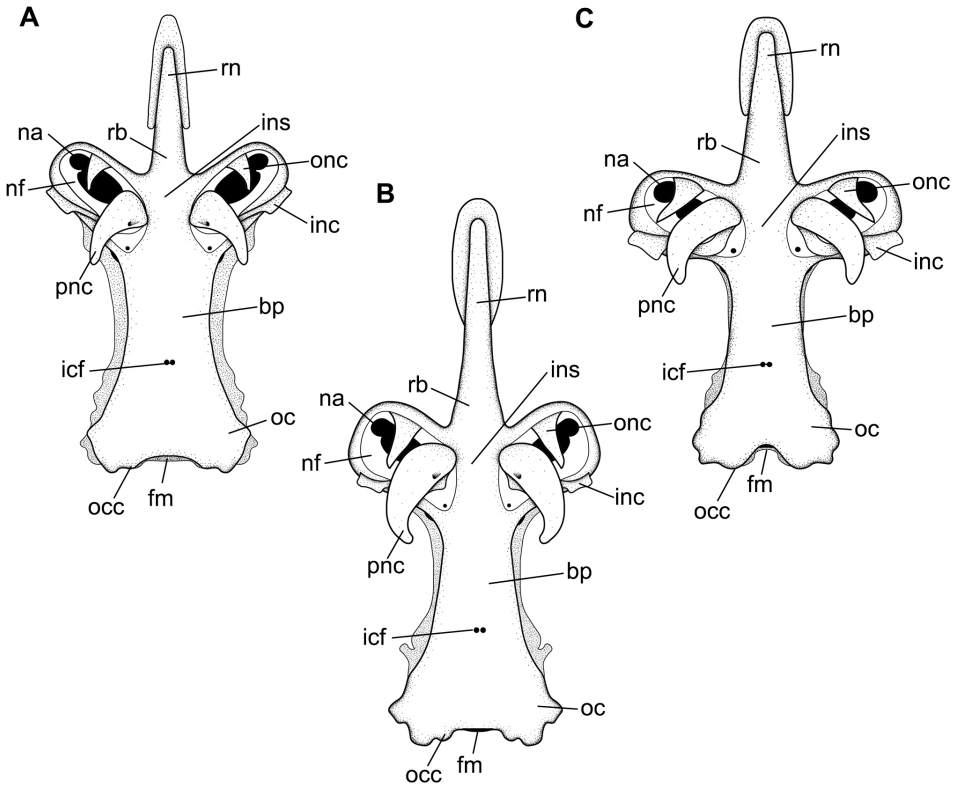

FIGURE 15 | Neurocranium of *Atlantoraja* species, ventral view. **A**, *A. castelnaui*, UERJ 1853, male, 593 mm TL. **B**, *A. cyclophora*, MNRJ 117184, female, 583 mm TL. **C**, *A. platana*, UERJ 1383, male, 372 mm TL. **bp,** basal plate; **fm**, foramen *magnum;* **icf,** internal carotid artery foramen; **inc**, inner nasal cartilage; **ins**, internasal space; **na**, nasal aperture; **nf**, nasal fontanelle; **oc,** otic capsule; **occ**, occipital condyle; **onc**, outer nasal cartilage; **pnc**, posterior nasal cartilage; **rb**, rostral base; **rn**, rostral node.

half-length in *A. castelnaui*, and extending to the anterior edge of supraorbital crest. Posterior margin concave in *A. cyclophora* and *A. platana* while straight in *A. castelnaui*; no indentation observed. Epiphysial bridge long and corresponding to half-length of the anterior fontanelle and 5.3–7.3 times in the neurocranial length. Posterior fontanelle teardrop-shape in *A. cyclophora* and *A. platana*, and subrectangular in *A. castelnaui*, and corresponding to one-half to two-thirds of the length of anterior fontanelle. Preorbital process conspicuous and continuous to the supraorbital crest in *A. cyclophora* and *A. platana*, while inconspicuous or absent in *A. castelnaui*; postorbital process notched for the passage of infraorbital lateral line canal (Fig. 14).

Orbital region delimited anteriorly by the posterior margin of the nasal capsules, posteriorly by the anterior margin of otic capsules, dorsally by the cranial roof, ventrally by the basal plate, and medially by the orbital wall, which is perforated by several foramina to the passage of cranial nerves and blood vessels (Fig. 16). Oronasal canal ventrally situated close to the basal plate. The foramen for the anterior cerebral vein lies on the same vertical line between the oronasal canal and the foramina for the *ophtalmicus* nerve. A single foramen for the trochlear nerve (IV) lies anterior to the large foramen for the optic nerve (II) and dorsal to the foramen for the optic nerve in *A. castelnaui* and *A. platana* and on the same horizontal line to the the foramen for the optic nerve in *A.*

cyclophora. The position of the foramen of the optic nerve varies from anterior to the half-length of orbital wall in *A. cyclophora* and *A. platana* to slightly posterior to it in *A. castelnaui*. Foramen for the oculomotor nerve (III) posterior to the optic nerve but anterior to the half-length of orbital wall in *A. cyclophora* and more posteriorly situated in *A. castelnaui*. The optic pedicel lies ventrally to the foramen for the abducens nerve (VI) in *A. cyclophora* and *A. platana*, and between the foramina for the oculomotor and abducens nerves in *A. castelnaui*. The foramen for the abducens nerve lies more closely situated to the posterior margin than to the half-length of orbital wall in *A. castelnaui*. Foramen for the afferent pseudobranchial artery lies ventrally to the optic pedicel and close to the basal plate. The second largest aperture of the orbital wall is the foramen prootic for the passage of the *trigeminus* and *facialis* nerves (V+VII). Prootic foramen separated posteriorly from the hyomandibular *ramus* of the *facialis* nerve by the prefacial commissure, close to the otic region (Fig. 16).

Basal plate begins anteriorly at the ethmoidal fossa right after the nasal capsules, runs

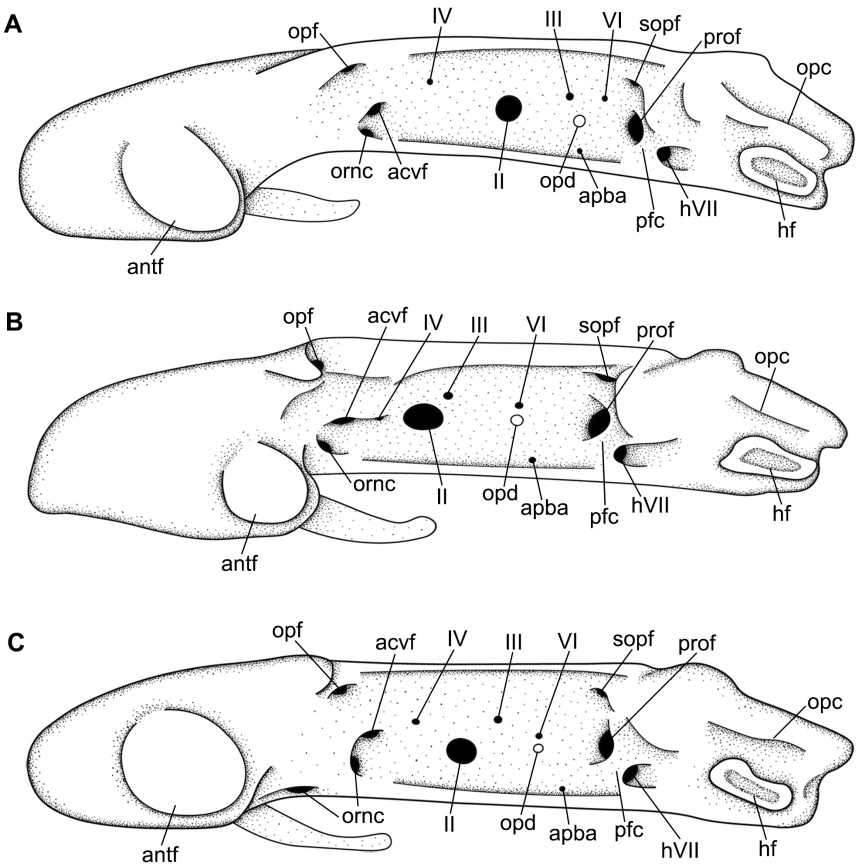

FIGURE 16 | Neurocranium of *Atlantoraja* species; lateral view. **A**, *A. castelnaui*, UERJ 1853, male, 593 mm TL. **B**, *A. cyclophora*, MNRJ 117184, female, 583 mm TL. **C**, *A. platana*, UERJ 1383, male, 372 mm TL. **II**, foramen for the optic nerve; **III**, foramen for the oculomotor nerve; **IV**, foramen for the trochlear nerve; **VI**, foramen for the abducens nerve; **acvf**, anterior canal vein foramen; **antf**, antorbital facet; **apba**, foramen for the afferent pseudobranchial artery; **hf**, hyomandibular facet**; hVII**, foramen for the passage of the hyomandibular *ramus* of the *facialis* nerve; **opc**, opistotic crest; **opd** ¸ optic pedicel; **opf**, ophthalmic foramen; **ornc** oronasal canal; **pfc**, prefacial commissure; **prof**, prootic formamen; **sopf**, superficial ophtalmic foramina.

to the posteroventral end of the optic region and ends at the ventral margin of the foramen *magnum*; ethmoidal fossa narrower in *A. cyclophora* and *A. platana* than in *A. castelnaui* (Fig. 15). Two internal carotid foramina ventrally situated, closely set and slightly anterior to the level of postorbital process.

Otic region as the second widest region of the neurocranium (Figs. 14–15), composed of otic capsules, impressions of semicircular canals, parietal fossa and foramina for the endolymphatic (smaller aperture) and perilymphatic canals. Opistotic crest well-developed and posterior to the sphenopterotic crest, running dorsally to the otic capsule and ending close to the occipital region. Hyomandibular facet elongate, slightly concave and obliquely positioned on lateral otic region, lined dorsally by the postorbital groove and jugal arch.

Occipital region consists in the posterior surface of the chondrocranium, composed of the large foramen magnum and the lateral edges of the hyomandibular facet. Occipital condyle situated on the lateral margin of the foramen *magnum* and lateral to it lies the foramen for the *vagus* nerve (X). Lateral to the foramen for the *vagus* nerve lies the foramen for the glossopharyngeal nerve (IX).

Jaws and teeth. Upper jaw slightly concave medially and strongly convex laterally; lower jaw strongly convex throughout its extension (Fig. 17). Both jaws tapering toward midline. Upper tooth row counts 40–49 and lower ones 37–45. Sexual heterodonty well pronounced with females presenting rounded and flattened tooth crowns and males presenting teardrop-shaped teeth on symphyseal region. Monognathic heterodonty observed only in male specimens (Fig. 18).

Hyoid and gill arches. Hyomandibular cartilage tapering anteriorly and articulating

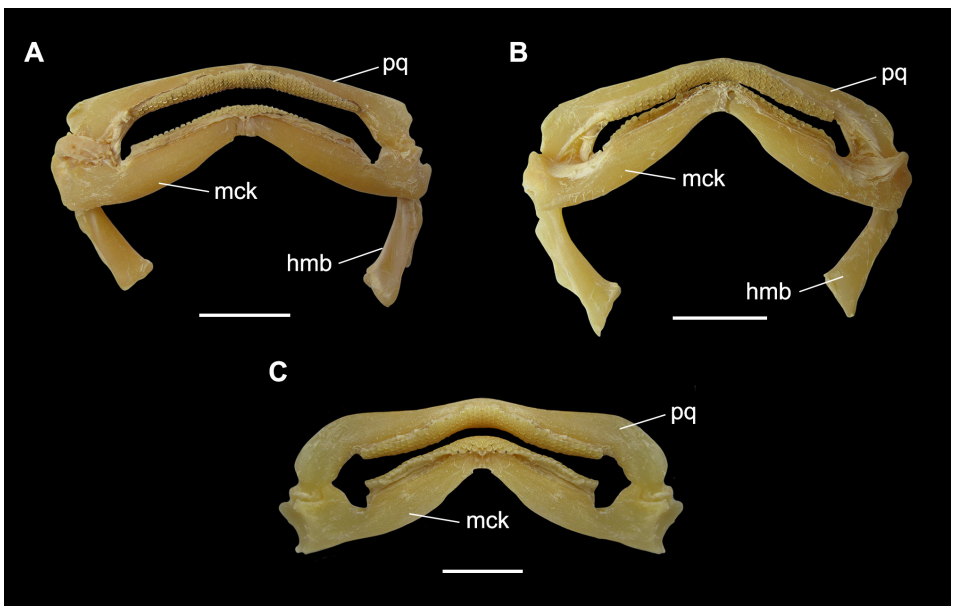

FIGURE 17 | Jaws and hyomandibular cartilage of *Atlantoraja* species. **A**, *A. castelnaui*., UERJ 1853, male, 593 mm TL. **B**, *A. platana*, UERJ 1383, male, 372 mm TL; **C**, *Atlantoraja cyclophora*, MNRJ 117184, female, 583 mm TL. **hmb**, hyomandibula; **mck**, Meckel's cartilage; **pq**, palatoquadrate. Scale bars = 20 mm.

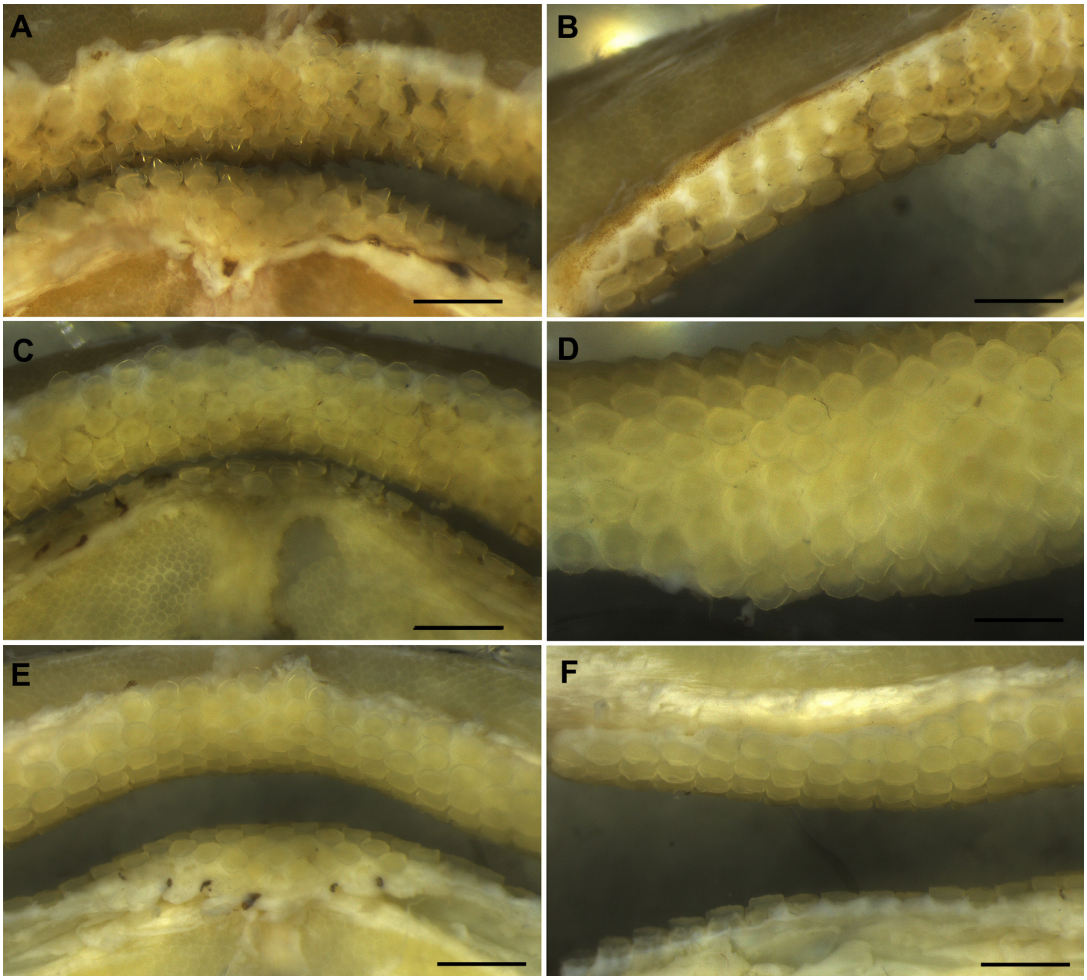

FIGURE 18 | Teeth of *Atlantoraja* species. **A.** Symphyseal region, **B.** Commissural region of *A. castelnaui*, UERJ 1853, male, 593 mm TL. **C.** Symphyseal region, **D.** Commissural region of *A. cyclophora*, MNRJ 117184, female, 583 mm TL. **E.** Symphyseal region, **F.** Commissural region of *A. platana*, UERJ 1383, male, 372 mm TL. Scale bars = 5 mm.

to the lateral surface of jaws (Fig. 17). Dorsal and ventral pseudohyoid rodlike and laterally situated to the basihyal cartilage. Basihyal wide and slender, slightly arched and with anterolateral projections; medially notched in *A. platana* (Fig. 19). Hypobranchials II small, trapezoidal and restricted to the medial portion of ceratobranchials I and II. Hypobranchials III and IV fused in *A. cyclophora* and *A. platana*, separated in *A. castelnaui*; not reaching the anterior portion of basibranchial copula. Ceratobranchials I–IV overlapping medially; ceratobranchial V articulating directly to the basibranchial copula. Epibranchials I and V longer than the medial ones. Pharyngobranchials II and III longer than the first; gill pickax short. Anterior processes of basibranchial copula long and similar in size to its posterior portion; laterally concave in *A. cyclophora* and *A. platana*, and nearly straight in *A. castelnaui* (Fig. 19). Basibranchial copula with rounded posterolateral margins in *A. cyclophora* and *A. platana* while nearly straight in *A. castelnaui*. Accessory cartilage of the basibranchial copula distinct, triangular and corresponding to one-fourth to one-third of the basibranchial copula.

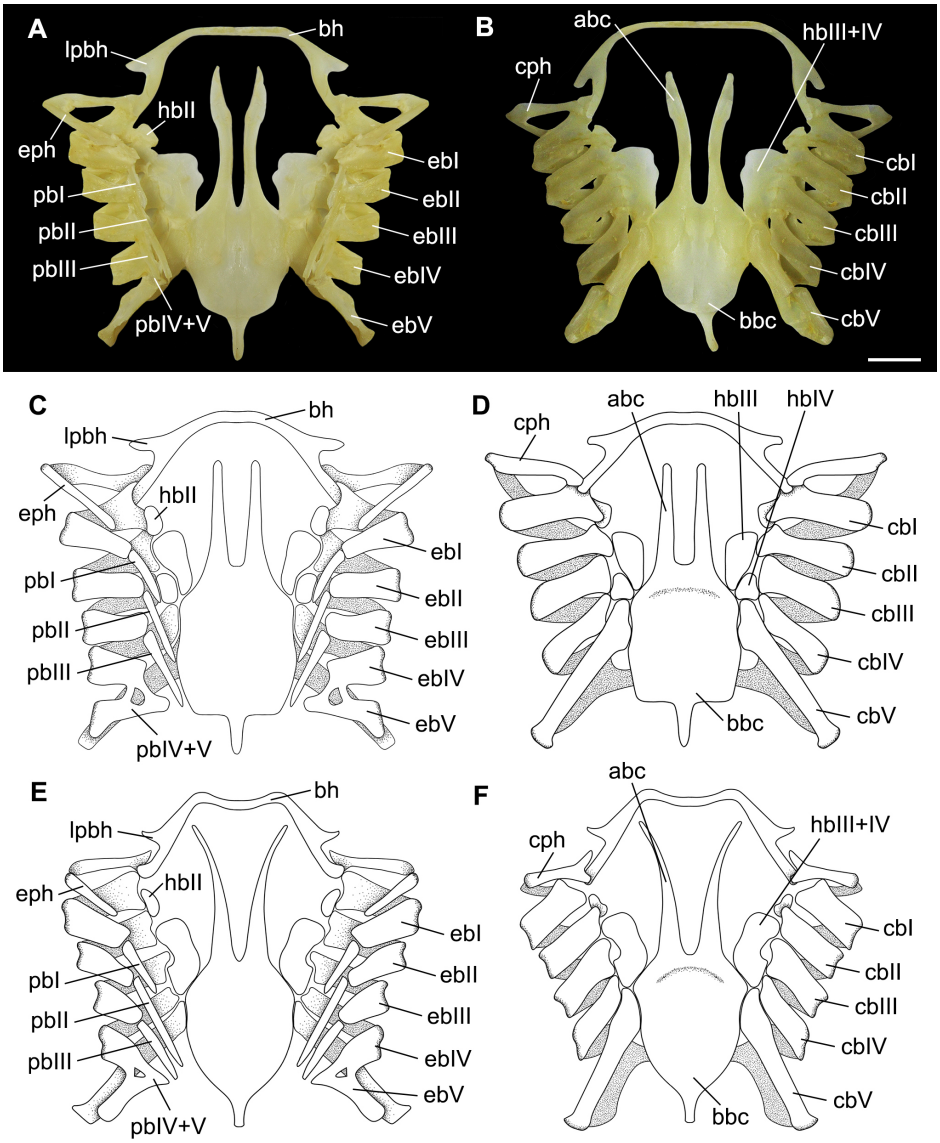

FIGURE 19 | Hyoid and gill arches of *Atlantoraja* species. **A**, **B.** *A. cyclophora*, MNRJ 117184, female, 583 mm TL. **C**, **D**. *A. castelnaui*, UERJ 1853, male, 593 mm TL. **E**, **F.** *A. platana*, UERJ 1383, male, 372 mm TL. **abc**, anterior portion of basibranchial copula; **bbc**, basibranchial copula; **bh**, basihyal; **cb I-V** ceratobranchials I-V; **cph**, cerato-pseudohyoid; **eb I-V**, epibranchials I-V; **eph**, epi-pseudohyoid; **hb II-IV**, hypobranchials II-IV; **lpbh**, lateral projection of basihyal; **pb I-V**, pharyngobranchials I-V. Scale bar = 10 mm.

Pelvic girdle and fin. Pelvic bar transverse and nearly straight, with lateral prepelvic processes triangular and directed anteriorly from the outer corner at each end (Fig. 20). Median ischio-pubic region and lateral iliac regions, penetrated by the obturatorial nerve foramina for the passage of the diazonal nerves. Condyle for articulation with enlarged first anterior radial situated ventrolaterally; obturator foramina posterior to the puboischiac condyle. Pelvic anterior lobe with six or seven segments; first one stout and elongate with very concave articular surface for puboischiac condyle. Posterior lobe with 17–20 radial segments.

DISCUSSION

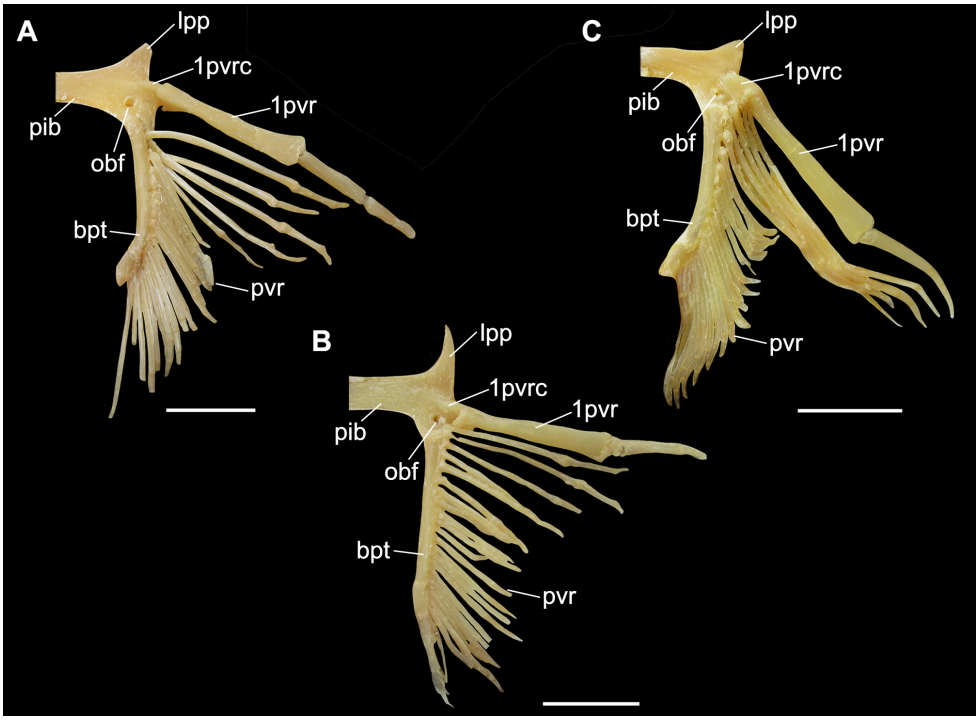

FIGURE 20 | Pelvic girdle and fin of *Atlantoraja* species. **A.** *A. castelnaui*., UERJ 1853, male, 593 mm TL. **B.** *A. cyclophora*, MNRJ 117184, female, 583 mm TL. **C.** *A. platana*, UERJ 1383, male, 372 mm TL. **1pvr**, first pelvic radial segment; **1pvrc,** condyle for the first pelvic radial segment; **bpt**, basipterygium; **obf**, obturator foramen; **lpp**, lateral pelvic process; **pib**, pubischiac bar; **pvr**, pelvic radial segments. Scale bars = 20 mm.

Differences among species of *Atlantoraja* are found mainly in neurocranial morphology, squamation, coloration and maturity size. According to our observations, *Atlantoraja cyclophora* and *A. platana* are more similar to each other than to *A. castelnaui* in regards to their smoother dorsal surface, position of orbital foramina, overall shape of neucrocranium, presence of dark blotches or ocelli on the medial region of pectoral fin dorsal surface and body measurements (Tab. 8). In addition, Gomes *et al*. (1997) reported some differences in the morphology of the synarchual cartilage with a greater number of spinal foramina in dorsal and ventral roots and cervic-thoracic vertebrae centra in *A. castelnaui* than in *A. cyclophora* and *A. platana* (41 *vs*. 32–36 and 9 *vs*. 6–8, respectively). Also, the dorsal margin of the anterior lateral flap of the synarchual is undulated in *A. castelnaui* (Gomes *et al*., 1997:98, fig. 5) while it is slightly convex in *A. cyclophora* (fig. 7) and *A. platana* (fig. 6). In relation to egg capsule morphology, *A. castelnaui* differs from the other two by the absence of longitudinal striae on the egg surface, being smooth to touch (Oddone, Vooren, 2008).

A close relationship between *A. cyclophora* and *A. platana* was already hypothesized by previous studies (Barbosa, Gomes, 1998; Naylor *et al*., 2012; Coelho *et al*., 2020), however, clasper morphology seems to contradict this arrangement. Clasper external morphology of *Atlantoraja cyclophora* is markedly distinct from *A. castelnaui* and *A. platana* by the presence of proximal and distal clefts, eperon, pseudorhipidion and grip component (Moreira *et al*., 2017). Furthermore, *Atlantoraja castelnaui* and *A. platana*

TABLE 8 | Summary of morphological differences observed among *Atlantoraja* species.

Characters	*A. castelnaui*	*A. cyclophora*	*A. platana*
Body dorsal surface	Densely covered by prickles and thorns	Smooth	Smooth
Nasal capsule	Strongly oblique to the anteroposterior axis	Slightly oblique to the anteroposterior axis	Perpendicular to the anteroposterior axis
Anterior region of cranial roof	Broad	Slender	Slender
Anterior extension of anterior fontanelle	Half-length of rostral cartilage	Posterior fourth of rostral cartilage	Posterior fourth of rostral cartilage
Posterior fontanelle	Subrectangular	Teardrop-shaped	Teardrop-shaped
Preorbital process	Inconspicuous	Conspicuous	Conspicuous
Foramen for the trochlear nerve (IV)	Dorsal to the foramen for the optic nerve (II)	On the same line of foramen for the optic nerve (II)	Dorsal to the foramen for the optic nerve (II)
Foramen of the optic nerve (II)	Posterior to half-length of orbital wall	Anterior to half-length of orbital wall	Anterior to half-length of orbital wall
Optic pedicel	Between the foramina for oculomotor and the abducens nerves	Ventral to the foramen for the abducens nerve (VI)	Ventral to the foramen for the abducens nerve (VI)
Foramen for the abducens nerve (VI)	Closer to the posterior margin of orbital wall	Closer to the half-length of orbital wall	Closer to the half-length of orbital wall

possess spike components on their claspers, which are absent in *A. cyclophora* (Moreira *et al*., 2017). Regarding skeletal clasper components, all three *Atlantoraja* species share a dorsal terminal 1 cartilage with inverted U-shape and a dorsal terminal 2 cartilage extended proximally to the dorsal marginal cartilage, both proposed as diagnostic characters for the genus (Menni, 1972; Moreira *et al*., 2017; present study). Given the relevance of clasper features for the systematics of the tribe Riorajini, characters from this anatomical complex as well as from external morphology and internal anatomy presented here need to be included in a phylogenetic analysis and tested cladistically in order to better understand the interrelationships within this clade and also among Riorajini species and other arhynchobatids.

ACKNOWLEDGMENTS

The authors wish to thank Calorus Vooren (*in memoriam*) and Maria Cristina Oddone (FURG), Gustavo Chiaramonte (MACN), Carlos Lucena and Margarete Lucena (MCP), Paulo Buckup, Cristiano Araújo, Mariane Targino (MNRJ), Bernard Séret (MNHN) and José Lima Figueiredo, Alessio Datovo (MZUSP) for permission to examine specimens under their care. To Cristiano Araújo (MNRJ) and James Maclaine (BMNH) for sending photographs of type specimens. To Hugo Santos for all the help and valuable comments for this study. The first author was supported by CAPES (Finance code 001).

REFERENCES

- **Andreata JV, Séret B.** Relação dos peixes coletados nos limites da plataforma continental e nas montanhas submarinas Vitória, Trindade e Martin Vaz, durante a campanha oceanográfica MD-55 Brasil. Rev Bras Zool. 1995; 12(3):579–94. https://doi.org/10.1590/S0101-81751995000300014
- **Barbosa FS, Gomes UL.** Morfologia juvenil de quatro espécies do gênero *Raja* (Linnaeus, 1958) das regiões sudeste e sul do Brasil (Chondrichthyes, Batoidei, Rajidae). Biociências. 1998; 6(2):125–46.
- **Begossi A, Figueiredo JL.** Ethnoichthyology of southern coastal fishermen: cases from Búzios Island and Sepetiba Bay (Brazil). Bull Mar Sci. 1995; 56(2):710–17.
- **Bellisio NB, López RB, Torno A.** Peces marinos patagónicos. Buenos Aires: Editorial Códex; 1979.
- **Bernardes RA, Figueiredo JL, Rodrigues AR, Fischer LG, Vooren CM, Haimovici M, Rossi-Wontschowski CLDB.** Peixes da Zona Econômica Exclusiva da Região Sudeste-Sul do Brasil. Levantamento com armadilhas, pargueiras e rede de arrasto de fundo. São Paulo: Universidade de São Paulo; 2005.
- **Bigelow HB, Schroeder WC.** Fishes of the Western North Atlantic. Sawfishes, guitarfishes, skates and ray. Part two. Memoir Sears Foundation for Marine Research. New Haven: Yale University Press; 1953.
- **Bigelow HB, Schroeder WC.** New and little known batoid fishes from the western Atlantic. Bull Mus Comp Zool. 1961; 128(4):162–244.
- **Cappetta H.** Handbook of Paleoichthyology, Vol. 3E: Chondrichthyes – Mesozoic and Cenozoic Elasmobranchii: Teeth. München: Verlag Dr. Friedrich Pfeil; 2012.
- **Coelho JFR, Lima SMQ, Petean FF.** Phylogenetic conservatism of abiotic niche in sympatric Southwestern Atlantic skates. Mar Biol Res. 2020; 16(6–7):458–73. https://doi.org/10.1080/17451000.2020.1837883
- **Compagno LJV.** Checklist of living elasmobranchs. In: Hamlett WC, editor. Sharks, skates, and rays, the biology of elasmobranch fishes. Baltimore: John Hopkins University Press; 1999. p.471–98.
- **Compagno LJV.** Checklist of living Chondrichthyes. In: Hamlett WC, editor. Reproductive biology and phylogeny of chondrichthyes: sharks, rays and chimaeras. Endfield: CT Science Publishers; 2005. p.503–48.
- **Compagno LJV, Dando M, Fowler S.** Sharks of the World. Princeton: Princeton University Press; 2005.
- **Cousseau MB, Figueroa DE, Astarloa JMD.** Clave de identificación de las rayas del litoral marítimo de Argentina y Uruguay (Chondrichthyes, Familia Rajidae). Mar del Plata: INIDEP; 2000.
- **Cousseau MB, Figueroa DE, Astarloa JMD, Mabragaña E, Lucifora LO.** Rayas, chuchos y otros batoideos del Atlántico Sudoccidental (34º S-55º S). Mar del Plata: INIDEP; 2007.
- **Devincenzi GJ.** Peces del Uruguay. An Mus Nac Hist Nat Montev. 1920; 1(4):97–134.
- **Ebert DA, Compagno LJV.** Biodiversity and systematics of skates (Chondrichthyes: Rajiformes: Rajoidei). Environ Biol Fishes. 2007; 80(2–3):111–24. https://doi.org/10.1007/s10641-007-9247-0
- **Evermann BW, Kendall WC.** Notes on a collection of fishes from Argentina, South America, with descriptions of three new species. Proc U S Nat Mus. 1907; 31(1482):67–108.
- **Figueiredo JL.** Manual de peixes do sudeste do Brasil. I. Introdução, cações, raias e quimeras. São Paulo: Museu de Zoologia da Universidade de São Paulo; 1977.
- **Fowler HW.** Notes on batoid fishes. Proc Acad Nat Sci Phila. 1910; 62(2):468–75. Available from: https://www.jstor.org/stable/4063435
- **Gadig OBF.** Peixes cartilaginosos da costa do estado de São Paulo. Rev Ceciliana. 1998; 8(9):41–52.
- **Gadig OBF, Gomes UL.** Scyliorhinidae. In: Menezes NA, Buckup PA, Figueiredo JL, Moura RL, editors. Catálogo das espécies de peixes marinhos do Brasil. São Paulo: Museu de Zoologia da Universidade de São Paulo, 2003; 21–22.
- **Garman S.** The Plagiostomia (sharks, skates, and rays). Mems Mus Comp Zool. 1913; 36:1–515.

- **Gillis JA, Dahn RD, Shubin NH.** Chondrogenesis and homology of the visceral skeleton in the little skate, *Leucoraja erinacea* (Chondrichthyes: Batoidea). J Morphol. 2009; 270(5):628–43. https://doi.org/10.1002/jmor.10710
- **Gomes UL.** Revisão taxonômica da família Rajidae no Brasil (Chondrichthyes, Elasmobranchii, Rajiformes). PhD thesis, Universidade Federal do Rio de Janeiro. 2002
- **Gomes UL, Paragó C.** A utilização da distribuição de poros de canais de muco e da coloração ventral como caracteres taxonômicos em Riorajini (Chondrichthyes, Batoidea, Rajidae). Biociencias. 2005; 13(1):55–62.
- **Gomes UL, Santos HRS, Gadig OBF, Signori CN, Vicente MM.** Guia para identificação dos tubarões, raias e quimeras do Rio de Janeiro (Chondrichthyes: Elasmobrachii e Holocephali). Rev Nord Biol. 2019; 27(1):171–368. https://doi.org/10.22478/ufpb.2236-1480.2019v27n1.47122
- **Gomes UL, Signori CN, Gadig OBF, Santos HRS.** Guia de identificação de tubarões e raias do Rio de Janeiro. Rio de Janeiro: Technical Books; 2010.
- **Gomes UL, Winkelstein C, Souza-Lima W.** Estudo da cartilagem sinarcual cérvico-torácica em rajídeos (Batomorphii, Rajiformes) da região sudeste do Brasil. An Acad Bras Cienc. 1997; 69(1):95–107.
- **Günther A.** Report on the shore fishes procured during the voyage of H. M. S. Challenger in the years 1873–1876. Zoology. 1880; 1(6):1–82.
- **Hubbs CL, Ishiyama R.** Methods for the taxonomic study and description of skates (Rajidae). Copeia. 1968; 1968(3):483–91. https://doi.org/10.2307/1442016
- **Hulley PA.** The origin, interrelationships and distribution of southern African Rajidae (Chondrichthyes, Batoidea). Ann S Afr Mus. 1972; 60:1–103.
- **Knoff M, Clemente SCS, Pinto RM, Gomes DC.** Nematodes of elasmobranch fishes from the southern coast of Brazil. Mem Inst Oswaldo Cruz. 2001; 96(1):81–87. https://doi.org/10.1590/S0074-02762001000100009
- **Last PR, Stehmann MFW, Séret B, Weigmann S.** Soft-nose skates. Family Arhynchobatidae. In: Last PR, White WT, Carvalho MR, Séret B, Stehmann MFW, Naylor GJP, editors. Rays of the world. Melbourne: CSIRO Publishing; 2016. p.364–472.
- **Leible M.** Revisión de métodos para estudios taxonómicos de rayas (Rajiformes, Rajidae). Gayana (Concepc). 1988; 52(102):15–93.
- **Leigh-Sharpe WH.** The comparative morphology of the secondary sexual characters of elasmobranch fishes. The claspers, clasper siphons, and clasper glands. Memoir VII. J Morph. 1924; 39(2):567–77. https://doi.org/10.1002/jmor.1050390211
- **Lessa R, Santana FM, Rincón G, Gadig OB, El-Deir ACA.** Biodiversidade de Elasmobrânquios do Brasil. Relatório para o Programa Nacional de Diversidade Biológica (PRONABIO). Brasília: MMA; 1999.
- **Lopes PRD.** Catálogo dos peixes marinhos do Laboratório de Ictiologia da Universidade Federal do Rio de Janeiro. Parte I: Chondrichthyes (Rajiformes). Teleostei (Elopiformes a Dactylopteriformes). Rev Bras Zool. 1989; 6(2):201–17. https://doi.org/10.1590/S0101-81751989000200004
- **Lucena CAS, Lucena ZMS.** Catálogo dos peixes marinhos do Museu de Ciências da Pontifícia Universidade Católica do Rio Grande do Sul. Elasmobranchiomorphii. Teleostomi (1a parte). Comun Mus Ciênc Tecnol PUCRS, Sér Zool. 1981; 21:1–66.
- **Marini TL.** Enumeración de los peces coleccionados en las inmediaciones del Laboratorio de Biologia Marina de Puerto Quenquén. Physis, Buenos Aires. 1929; 9(34):451–54.
- **Mazzoleni RC, Schwingel PR.** Elasmobranch species landed in Itajaí Harbour, Southern Brazil. Notas Tec Facimar. 1999; 3:111–18.
- **McEachran JD, Compagno LJV.** A further description of *Gurgesiella furvescens* with comments on the interrelationships of Gurgesiellidae and Pseudorajidae (Pisces, Rajoidei). Bull Mar Sci. 1979; 29(4):530–53.

Neotropical Ichthyology

OPEN ACCESS

SBI | Official Journal of the Sociedade Brasileira de Ictiologia

- **McEachran JD, Dunn KA.** Phylogenetic analysis of skates, a morphologically conservative clade of elasmobranchs (Chondrichthyes, Rajidae). Copeia. 1998; 1998(2):271–90. https://doi.org/10.2307/1447424
- **McEachran JD, Miyake T.** Phylogenetic interrelationships of skates: a working hypothesis (Chondrichthyes, Rajoidei). In: Pratt HL, Gruber SH, Taniuchi T, editors. Elasmobranchs as living resources: advances in the biology, ecology, systematics, and the status of the fisheries. Springfield: NOAA Technical Report NMFS; 1990. p.285–304.
- **Meneses P, Paesch L.** Guía de campo para la identificación de peces cartilaginosos en el Río de la Plata y su frente oceánico. Frente Marítimo. 2003; 19:145–94.
- **Menni RC.** *Raja* (*Atlantoraja*) subgen. nov. y lista critica de los Rajidae Argentinos (Chondrichthyes, Rajiformes). Rev Mus La Plata Zool. 1972; 11(103):165–73.
- **Menni RC.** Rajidae del litoral bonaerense I. Especies de los generos *Raja*, *Bathyraja* y *Sympterygia* (Chondrichthyes). Physis. 1973; 32(85):413–39.
- **Menni RC, Ringuelet RA, Arámburu RH.** Peces marinos de la Argentina y Uruguay. Reseña histórica, clave de famílias, género y especies, catálogo crítico. Buenos Aires: Editorial Hemisferio Sur; 1984.
- **Menni RC, Stehmann M.** Distribution, environment and biology of batoid fishes off Argentina, Uruguay and Brazil. A review. Rev Mus Argentino Cienc Nat. 2000; 2(1):69–109.
- **Miranda Ribeiro A.** Pescas do "Annie". Bol Soc Nac Agr. 1903; (4–7):1–53.
- **Miranda Ribeiro A.** Fauna brasiliense. Peixes II. Desmobranchios. Arq Mus Nac. 1907; 14:131–217.
- **Miranda Ribeiro A.** Fauna brasiliense. Peixes (vol. 2). Rio de Janeiro: Imprensa Nacional; 1923.
- **Miranda Ribeiro P.** Tipos das espécies e subespécies do Prof. Alipio de Míranda Ribeiro depositados no Museu Nacional. Arq Mus Nac. 1953; 42:389–417.
- **Miranda Ribeiro P.** Catálogo dos peixes do Museu Nacional. IV. Chimaerdoides. Elasmobranquios. Publicações Avulsas do Museu Nacional. 1959; 32:1–12.
- **Miranda Ribeiro PM.** Pesca do Toku Maru. Bol Mus Nac Zool Rio de Janeiro. 1961; 288:1–18.
- **Moreira RA, Gomes UL, Carvalho MR.** Clasper morphology of skates of the tribe Riorajini (Chondrichthyes: Rajiformes: Arhynchobatidae) and its systematic significance. J Morph. 2017; 278(9):1185–96. https://doi.org/10.1002/jmor.20703
- **Naylor GJP, Caira JN, Jensen K, Rosana KAM, Straube N, Lakner C.** Elasmobranch phylogeny: a mitochondrial estimate based on 595 species. In: Carrier JC, Musick JA, Heithaus MR, editors. Biology of sharks and their relatives. Florida: CRC Press; 2012. p.31–56.
- **Nishida K.** Phylogeny of the suborder Myliobatidoidei. Memoirs Fac Fish Hokkaido Univ. 1990; 37(1–2):1–108.
- **Oddone MC, Amorim AF.** Length-weight relationships, condition and population sructure of the genus *Atlantoraja* (Elasmobranchii, Rajidae, Arhynchobatinae) in Southeastern Brazilian waters, SW Atlantic Ocean. J Northw Atl Fish Sci. 2007; 38:43–52. http://dx.doi.org/10.2960/J.v38.m599
- **Oddone MC, Amorim AF.** Size maturity of *Atlantoraja platana* (Günther, 1880) (Chondrichthyes: Rajidae: Arhynchobatinae) in the south-west Atlantic Ocean. J Fish Biol. 2008; 72(6):1515–19. https://doi.org/10.1111/j.1095-8649.2007.01774.x
- **Oddone MC, Amorim AF, Mancini PL.** Reproductive biology of the spotback skate, *Atlantoraja castelnaui* (Ribeiro, Rajidae), in southeastern Brazilian waters. Rev Biol Mar Oceanogr. 2008; 43(2):327–34. Available from: http://repositorio.furg.br/handle/1/1235
- **Oddone MC, Marçal AS, Vooren CM.** Egg capsules of *Atlantoraja cyclophora* (Regan, 1903) and *A. platana* (Günther, 1880) (Pisces, Elasmobranchii, Rajidae). Zootaxa. 2004; 426(1):1–04. https://doi.org/10.11646/zootaxa.426.1.1
- **Oddone MC, Paesch L, Norbis SW.** Size at first sexual maturity of two species of rajoid skates, genera *Atlantoraja* and *Dipturus* (Pisces, Elasmobranchii, Rajidae) from the Southwestern Atlantic (Pisces, Elasmobranchii, Rajidae) from the Southwestern Atlantic Ocean. J Appl Icht. 2005; 21(1):70–72. https://doi.org/10.1111/j.1439-0426.2004.00597.x

- **Oddone MC, Amorim AF.** Length-weight relationships, condition and population sructure of the genus *Atlantoraja* (Elasmobranchii, Rajidae, Arhynchobatinae) in Southeastern Brazilian waters, SW Atlantic Ocean. J Northw Atl Fish Sci. 2007; 38:43–52. http://dx.doi.org/10.2960/J.v38.m599
- **Oddone MC, Velasco G.** Relationship between liver weight, body size and reproductive activity in *Atlantoraja cyclophora* (Elasmobranchii: Rajidae: Arhynchobatinae) in oceanic waters off Rio Grande do Sul, Brazil. Neotrop Biol Conserv. 2006; 1(1):12–16. Available from: http://revistas.unisinos.br/index.php/neotropical/article/view/6193
- **Oddone MC, Vooren CM.** Distribution and abundance of *Atlantoraja cyclophora* (Regan, 1903) (Elasmobranchii, Rajidae) with regard to salinity, temperature and depth in southern Brazil, south-western Atlantic. Neotrop Ichthyol. 2004; 2(3):137–44. https://doi.org/10.1590/S1679-62252004000300005
- **Oddone MC, Vooren CM.** Reprodutive biology of *Atlantoraja cyclophora* (Regan, 1903) (Elasmobranchii: Rajidae) off southern Brazil. ICES J Mar Sci. 2005; 62(6):1095–103. https://doi.org/10.1016/j.icesjms.2005.05.002
- **Oddone MC, Vooren CM.** Comparative morphology and identification of egg capsules of skate species of the genera *Atlantoraja* Menni, 1972, *Rioraja* Whitley, 1939, and *Sympterygia* Müller & Henle, 1837. Arquivos Ciências do Mar. 2008; 41(2):5–13.
- **Pollom R, Barreto R, Charvet P, Chiaramonte GE, Cuevas JM, Faria V, Herman K, Motta F, Paesch L, Rincon G.** *Atlantoraja castelnaui*. The IUCN Red List of Threatened Species. 2020a; e.T44575A152015479. https://dx.doi.org/10.2305/IUCN.UK.2020-3.RLTS.T44575A152015479.en
- **Pollom R, Barreto R, Charvet P, Chiaramonte GE, Cuevas JM, Faria V, Montealegre-Quijano S, Motta F, Paesch L.** *Atlantoraja cyclophora*. The IUCN Red List of Threatened Species [Internet]. 2020b; e.T61398A3103491. https://dx.doi.org/10.2305/IUCN.UK.2020-3.RLTS.T61398A3103491.en
- **Pollom R, Barreto R, Charvet P, Chiaramonte GE, Cuevas JM, Faria V, Herman K, Montealegre-Quijano S, Motta F, Paesch L, Rincon G.** *Atlantoraja platana*. The IUCN Red List of Threatened Species [Internet]. 2020c; e.T63110A3118881. https://dx.doi.org/10.2305/IUCN.UK.2020-3.RLTS.T63110A3118881.en
- **Regan CT.** On a collection of fishes made by Dr. Goeldi at Rio Janeiro. Proc Zool Soc Lond. 1903; 1903(2):59–68.
- **Ringuelet RA, Aramburu RH.** Peces Marinos de la Republica Argentina. Clave para el reconocimento de famílias y gêneros. Buenos Aires: Agro Publ Tecn; 1960.
- **Roux C.** Poisson chondrichthyens du plateau continental brésilien et du Rio de La Plata. Campagne de la Calypso au large des côtes atlantiques de l'Amérique du Sud (1960-1961). Annales de l'Institut Océanographique. 1979; 55(11):111–30.
- **Ruschi A.** Lista dos tubarões, raias e peixes de água doce e salgada do Estado do Espírito Santo e uma observação sobre a introdução do dourado no Rio Doce. Bol Mus Biol Prof Mello Leitão. 1965; 25:1–23.
- **Sadowsky V, Menni RC.** Sobre *Raja platana* Gunther, 1880 (Chondricthyes, Rajidae). Physis. 1974; 33(86):23–32.
- **Silva KCR, Oddone MC.** Variação ontogenética da dentição da raia-pintada *Atlantoraja castelnaui* (Miranda-Ribeiro, 1907) (Chondrichthyes, Archynchobatidae). Bol Soc Zool Urug. 2020; 29(1):1–12. https://doi.org/10.26462/29.1.1
- **Soares KDA, Gomes UL, Santos HRS.** Scapulocoracoid morphology in the skates of the tribe Riorajini (Elasmobranchii, Rajiformes, Arhynchobatidae). Zoomorphology. 2020; 139:493–500. https://doi.org/10.1007/s00435-020-00504-2
- **Soares KDA, Moreira RA, Gomes UL.** Redescription of the Rio skate *Rioraja agassizii* (Chondrichthyes: Rajiformes: Arhynchobatidae) with notes on internal anatomy and intraspecific variation. Neotrop Ichthyol. 2021; 19(2):e210059. https://doi.org/10.1590/1982-0224-2021-0059
- **Tomás ARG, Tutui SLS.** Identificação de carcaças de cações e raias da pesca comercial no Sudeste do Brasil. Ana Acad Bras Cienc. 1996; 68(4):583–91.

- **Uyeno T, Miyake T.** Rajidae. In: Uyeno T, Matsuura K, Fujii E, editors. Fishes trawled off Suriname and French Guiana. Tokyo: Japan Marine Fishery Resource Research Center; 1983. p.73–78.
- **Vooren CM.** Demersal elasmobranchs. In: Seelinger U, Odebrecht C, Castello JP, editors. Subtropical convergence environments: the coast and sea in the southwestern Atlantic. Berlin: Springer-Verlag; 1997. p.141–46.
- **Weigmann S.** Annotated checklist of the living sharks, batoids and chimaeras (Chondrichthyes) of the world, with a focus on biogeographical diversity. J Fish Biol. 2016; 88(3):837–1037. https://doi.org/10.1111/jfb.12874

AUTHORS' CONTRIBUTION

Karla D. A. Soares: Conceptualization, Data curation, Formal analysis, Funding acquisition, Investigation, Methodology, Software, Visualization, Writing-original draft, Writing-review and editing.

Renan A. Moreira: Conceptualization, Data curation, Formal analysis, Investigation, Methodology, Visualization, Writing-original draft, Writing-review and editing.

Rafael Fernandes Lopes da Silva: Data curation, Investigation, Methodology, Visualization, Writing-original draft, Writing-review and editing.

Ulisses L. Gomes: Conceptualization, Data curation, Formal analysis, Project administration, Supervision, Validation, Visualization, Writing-original draft, Writing-review and editing.

ETHICAL STATEMENTS

Not applicable.

COMPETING INTERESTS

The authors declare no competing interests.

HOW TO CITE THIS ARTICLE

- **Soares KDA, Moreira RA, Silva RFL, Gomes UL.** Taxonomy and morphology of the skate genus *Atlantoraja* (Rajiformes: Arhynchobatidae). Neotrop Ichthyol. 2021; 19(4):e210096. https://doi.org/10.1590/1982-0224-2021-0096

Neotropical Ichthyology

OPEN ACCESS

Official Journal of the
Sociedade Brasileira de Ictiologia
SBI